094527

ATAC RESOURCES LTD.

INDUCED POLARIZATION SURVEY AT THE NIKKI PROPERTY, SOUTHWESTERN YUKON TERRITORY

Mike Power, M.Sc. P.Geoph.

Location: 62° 3' N 140° 59' W
NTS: 115 K 02
Mining District: Whitehorse, YT
Date: 30 Nov 2004

SUMMARY

Induced polarization and resistivity surveys were conducted on the Nikki Property for ATAC Resources Ltd. to locate the source of gold and copper soil geochemical anomalies. A total of 15.1 line-km was surveyed with a pole-dipole array, using a 50 m dipole spacing and reading from the 1st to the 6th separation. The data was interpreted by employing automated computer inversion to generate 2D models of the chargeability and resistivity distribution along each line. These results were in turn contoured to generate a three dimensional model of the chargeability and resistivity distribution.

The survey located a central zone of low resistivity defined by an isosurface of material less than 200 ohm-m. At the western end of the survey grid, this central resistivity low is coincident with altered granodiorite containing limonite and sulphide mineralization. The central resistivity low narrow from 400 - 500 m wide on the west end to about 100 m wide on the east end. The low plunges to the east along strike across the grid but there is minor uplift and widening of the feature between the last two lines at the eastern end of the grid.

The central resistivity low is partially enveloped by a chargeability high defined by an isosurface enclosing material with chargeability in excess of 5 mV/V. This follows the north boundary of the resistivity low in the west and then passes under the resistivity low on the east. This enveloping chargeability high follow is peripheral to the granodiorite intrusion and is best developed in metasedimentary rocks. Where the enveloping chargeability high crosses beneath the central resistivity high, it follows a NW trend also apparent in the soil geochemical response. Portions of the enveloping chargeability high are coincident with the copper and gold soil geochemical response.

In addition to these two large scale features, the IP survey detected a number of anomalies likely caused by thin (< 25 m) tabular or podiform chargeable bodies of limited strike extent. These produced asymmetric, single slash and dipolar high amplitude chargeability highs and lows.

TABLE OF CONTENTS

LIST OF FIGURES

1.0 INTRODUCTION

Aurora Geosciences Ltd. was retained by ATAC Resources Ltd. to perform an induced polarization and resistivity (IP) survey at the Nikki Property south of Beaver Creek, Yukon Territory. The survey was conducted to locate the source of copper and gold geochemical anomalies on the property. A total of 15.1 line-km were covered during the IP survey. This report describes the survey, data processing and results, and contains an interpretation of the data.

2.0 LOCATION AND ACCESS

The Nikki Property is located 40 km south of Beaver Creek immediately east of the Canada / U.S. border in the Whitehorse Mining District. The property is centred at approximately 62° 3' N 140° 59' W on NTS 115 K 02 (Figure 1). The property is accessible by helicopter from staging points on the Alaska Highway, 15 km east of the property.

3.0 GRID

The location of the survey grid is shown in Figure 2. The geophysical survey was conducted over an existing soil grid. The lines were registered to geographic coordinates by taking repeated measurements with non-differential GPS receivers at stations spaced approximately 200 m along the lines. This data is appended to the report in a digital file.

4.0 PERSONNEL AND EQUIPMENT

The survey was conducted by the following personnel:

Crew chief:	Georges Belcourt, P.Geoph.
Technician:	Josh Melnyk
Helper:	Tyson Bourgard
Helper:	Dan Shorty

The crew was equipped with the following instruments and general equipment:

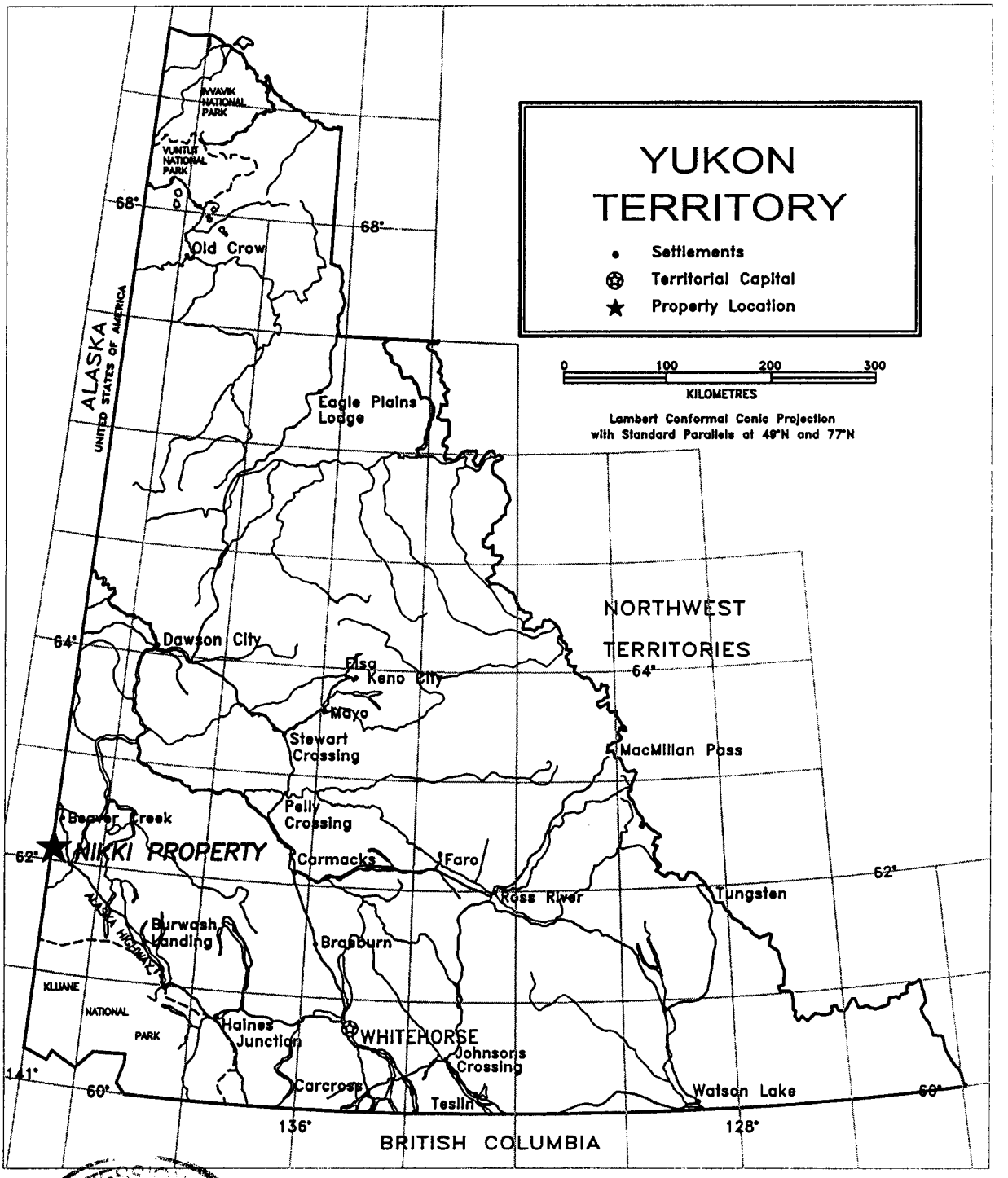

REGISTERED PROFESSIONAL GEOLOGIST
LICENSE
2010 May
N.W.T.

ATAC Resources Ltd.	NIKKI PROPERTY	
PROPERTY LOCATION MAP	MINING DISTRICT: WHITEHORSE	
	SCALE 1: 6,000,000	NTS: N/A
	DATUM: N/A	DRAWN BY: HDS
AURORA GEOSCIENCES LTD.	DATE: 29 November 04	FIGURE: 1

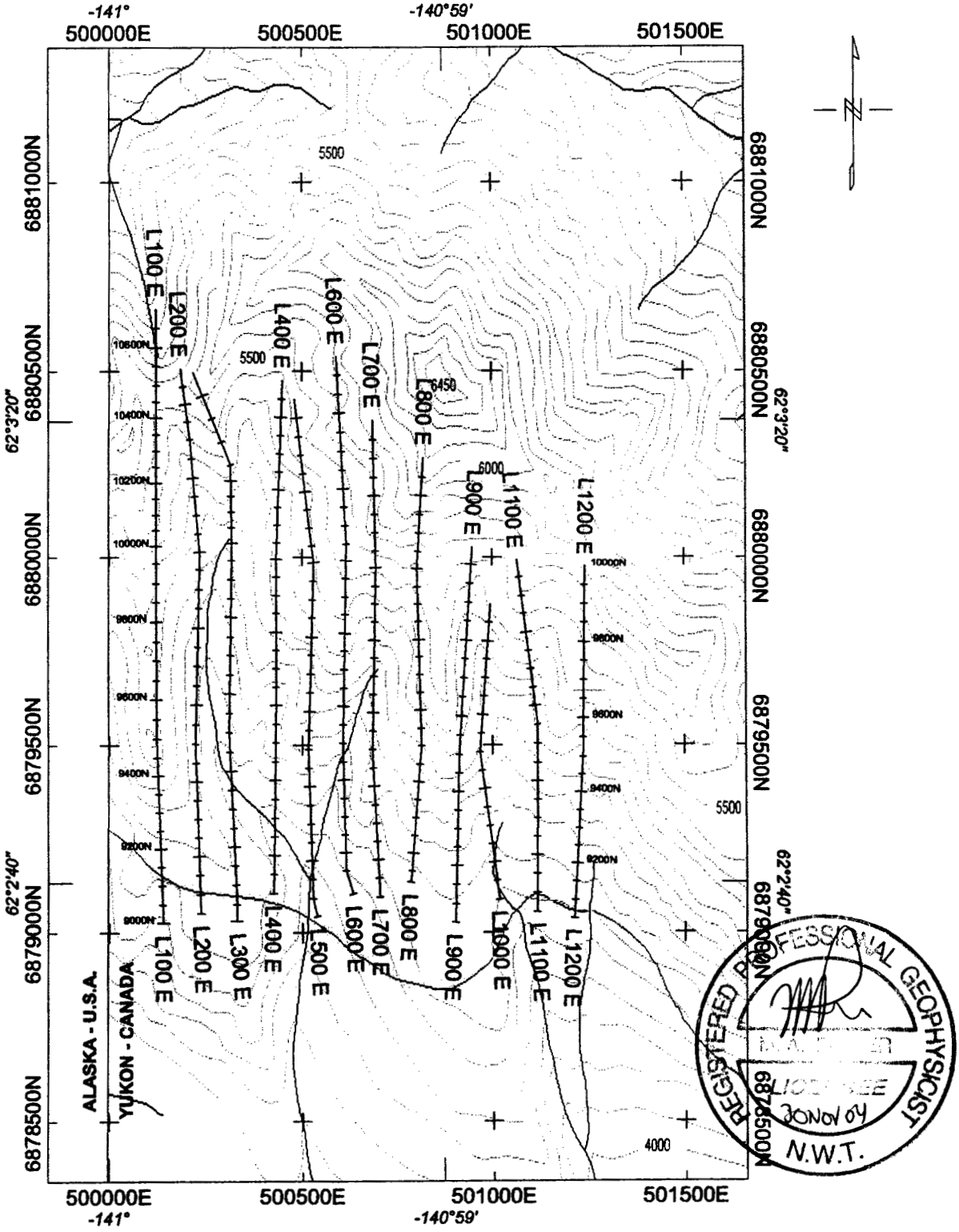

250 0 250
metres
Scale 1:16000
NAD83 / UTM zone 7N
Elevations in feet above mean sea level

ATAC RESOURCES LTD.	
NIKKI PROPERTY **IP SURVEY** **Figure 2. Grid Map**	
NTS: 115 K 02 Projection: UTM Zone 7N Job: ATAC-04-001 YT	Datum: NAD 83 Mining District: Whitehorse Date: 30 Nov 2004
AURORA GEOSCIENCES LTD.	

IP Transmitter:	GDD TX-II 3.5 KW digital IP transmitter s/n AGL64 Honda 5KVA gas generator
IP Receiver:	IRIS IP-6 digital 6-channel IP receiver s/n AGL63
Other IP equipment:	20 - 6 channel 50 m receiver cables 22 - stainless steel electrodes 6 km 18 gauge wire 2 - breast reels 2 - speedy winders 5 - VHF radios 1 - Spares kit and repair tools
Camp:	1 - 4 man summer camp (2 - 12'x14' tents, kitchen gear, generator, SAT phone)
Data processing:	Toshiba P 1.68GHz laptop Geosoft IP package

5.0 SURVEY SPECIFICATIONS

The survey was conducted according to the following specifications:

Array:	Pole-dipole
Dipole spacing:	50 m
Separations read:	n=1 to 6
Tx mode / signal:	Standard time domain signal (2 s +on, 2 s off, 2 s -on, 2 s off)
Receiver sampling:	Semi-logarithmic sampling of the decay curve in 20 windows, stacked minimum 15 times.
Parameters read:	M_t - total chargeability (ms) R_o - apparent resistivity M_1 to M_{10} - 10 channel samples of decay curve V_p - Primary voltage Sp - spontaneous potential E - error in chargeability (ms)

Noise: Standard deviation of the chargeability was kept to 5 ms or less wherever possible. If this was not possible, readings were repeated several times to determine their repeatability.

Other: Line end points were measured with non-differential GPS and station-to-station slopes were recorded with a clinometer to provide topography for the inversion.

6.0 SURVEY NOTES

The survey log in Appendix B describes survey operations including production. The crew mobilized to the property on August 24, 2004 by truck to White River and thence by helicopter to the property. The grid was surveyed from west to east and each line was surveyed from south to north with the infinite put in the low ground south of the grid. The stations were straight chained to accommodate the fixed length survey cables. The survey covered 15.0 line-km on 12 lines and was completed in 13 days. The crew demobilized on September 7, 2004 to Whitehorse.

7.0 IP INTERPRETATION METHOD

The data was interpreted using the DCIP2D package developed by the University of British Columbia Geophysical Inversion Facility. The inversion algorithm is described in detail by Oldenburg and Li (1994). A brief description of key features of the algorithm follows.

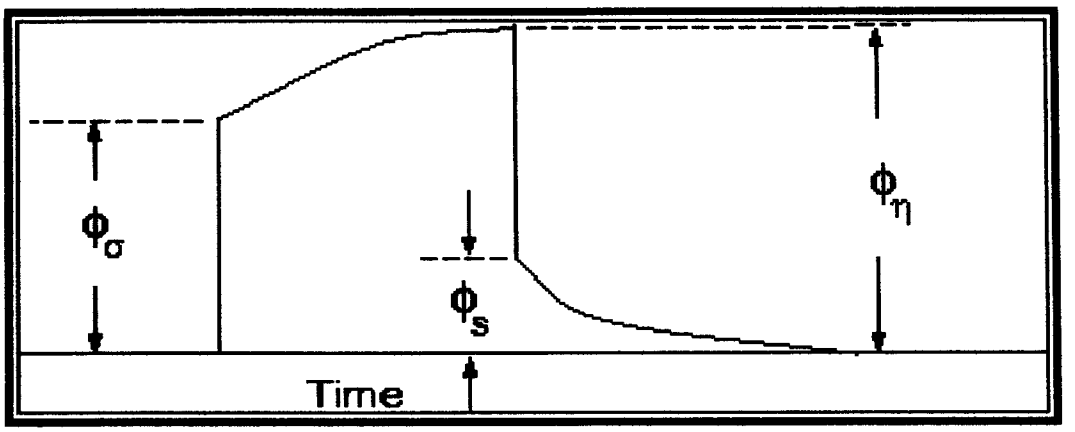

IP response curve (UBC DCIP2D documentation, 1998)

Siegel (1959) described the IP effect in macroscopic terms. If a time domain signal is put into the ground, as soon as the current is turned on, the voltage immediately rises to a level (ϕ_σ) and thereafter continues to rise to a higher level (ϕ_η). At current shutoff, the voltage immediately falls to a level (ϕ_s) and then slowly decays to zero along a curve similar to that between ϕ_σ and ϕ_η . Apparent chargeability is defined as the "extra" voltage observed:

$$\eta_a = \frac{\phi_\eta - \phi_\sigma}{\phi_\eta} = \frac{\phi_s}{\phi_\eta}$$

The observed DC potentials ϕ_σ are defined by the vector form of Ohms Law:

$$\nabla \cdot (\sigma \nabla \phi_s) = -I\delta(r - r_s)$$

where $\mathbf{r}-\mathbf{r}_s$ is the vector to the measurement point, **I** is the current and σ is the conductivity structure of the earth - the unknown quantity in the geophysical problem. The chargeability can be modeled by replacing the conductivity by an equivalent apparent conductivity controlled by the chargeability:

$$\sigma_\eta = \sigma(1 - \eta)$$

Modeling the IP effect then involves running two conductivity models - one with σ and

one with σ_η .

The unknown quantity is the distribution of conductivities in the earth. The software models the earth conductivity structure as a series of rectangular cells of varying size and aspect ratio. The grid is finest (most detailed) near the measurement points and much coarser at locations beside or at depth beneath the measurement points. The latter points are necessary to avoid having edge effects appear in the model. The size and dimensions of the models in no way compensates for the basic limitations on depth penetration and resolution inherent in the IP/resistivity survey. Thus the effective depth of penetration (0.5 to 1.0 times the maximum dipole separation) is the limit to which the models should be relied upon to accurately reflect true earth conductivities and chargeabilities.

The program calculates the potential across the finite element network using a starting model. Appropriate boundary conditions are applied when calculating the potentials across the network. These include the condition that all current flow is normal to the cell boundaries and voltages are continuous across the boundaries. The sensitivity of the model to changing the parameters in any cell is calculated as is the misfit between the model results and the actual observed potentials / chargeabilities. The model is then adjusted using the calculated sensitivities of the response to changes in the conductivity of individual cells.

There is no unique solution or model which fits any set of IP / resistivity data. A best-fit model is one which (1) minimizes misfit and (2) invokes the minimum required degree of complexity to fit the data. The minimization of misfit requires that the sum of the least squares differences between the field data and the data predicted by the model is minimized. For a set of **N** measurements, a global misfit can be defined as:

$$\Psi_d = \sum_{i=1}^{N} \left(W_i(r_i - r_i^{obs})\right)^2$$

where W_i is the weighting factor for the i^{th} measurement (r^{obs}) and r_i is the model response for this measurement. The weighting factor is usually in the order of the inverse of the expected error so that a measurement with high error has a low weighting and vice versa. In a system with no noise and perfectly determined errors, the global error would be **N** because the weighting would compensate for large spreads between model and observed results at points with large errors. The program minimizes Ψ_d by repeatedly adjusting the conductivities to improve the fit.

The second requirement of a successful solution is that the complexity of the final model be minimized. IP measurements are inherent averages, deriving resistivity and chargeabilities from large volumes of the subsurface. It is possible to over model data,

deriving solutions which minimize misfit but which invoke models with detail beyond the resolving power of the measuring arrays. Models which incorporate complex detail are inherently ambiguous in that they any number of such models, each with minor variations, may also minimize global misfit. The fine structures in models with extreme complexity exert little or no control on the overall model response. If both a simple and complex solution can adequately replicate the field data within the bounds of measurement error, the simple solution is to be preferred.

Starting with a reference model m_0 and weighting functions for x and z (w_x, w_z), define the complexity of the model as Ψ_m where:

$$\psi_m(m, m_0) = \alpha_s \int\int w_s(x,z)(m-m_0)^2\,dx\,dz + \int\int \left\{ \alpha_x w_x(x,z)\left(\frac{\partial(m-m_0)}{\partial x}\right)^2 + \alpha_z w_z(x,z)\left(\frac{\partial(m-m_0)}{\partial z}\right)^2 \right\} dx\,dz$$

where α_x, α_z and α_s define the relative weight of the model in x, z and fineness. Increasing any of these values beyond their normal values of 1.0, 1.0 and 0.001, increases the importance of that dimension in the final solution. For example, to weight the final solutions towards vertical structures, α_z would be weighted several times more than α_x. To force the model to generate fewer small scale structures, α_s is increased.

The final criteria for a successful solution can then be expressed as:

1. Minimize Ψ_m

2. Subject to the constraint that Ψ_d = N (or very close to it).

Consequently, the inversion process seeks to minimize two loosely related functions. To evaluate a solution, the reader should examine not only the final values but the path the program followed to reach these values. An example of typical convergence curves is shown below:

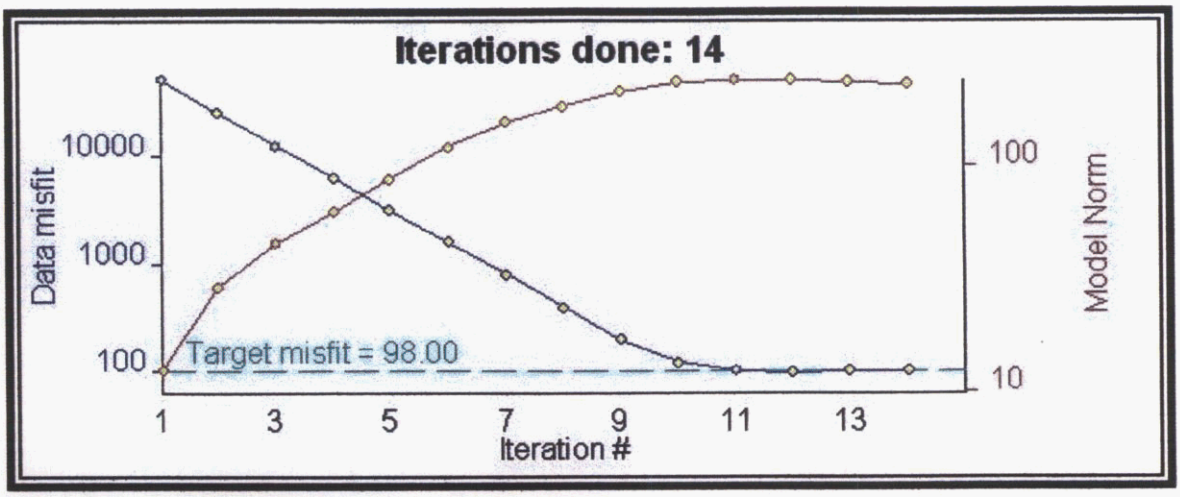

Typical convergence curves - DC inversion

The black line traces the value of Ψ_d with each iteration and in a good inversion, this will converge to the target misfit (N). The orange curve traces the convergence behavior of Ψ_m. This curve normally starts at a very small value because the reference model is usually set to the initial model and the initial and reference models are very simple. As the inversion proceeds, the solution model becomes increasingly complex as it is adjusted to meet the target misfit. After reaching target misfit, minor adjustments are made to reduce the complexity of the model and the Ψ_m curve stabilizes at some high value.

The field observations often have significant poorly quantified errors and the complexity of the background conductivity response may be such that it is impossible to reduce Ψ_d to N. Instead, Ψ_d can be scaled proportionately by a "chi-factor" ranging up or down from 1.0 (no scaling). Setting a large chi-factor loosens the control that goodness-of-fit exerts on the solution and generally directs the program to use very simple models which tend to smooth out the conductivities and fails to accurately model the fine details in resistivity or chargeability known to exist in the ground. Setting a chi-factor which is too low may prevent convergence to an acceptable solution. Generally, chi is left at 1.0.

A final feature of note in the inversion is the use of initial and reference conductivity and chargeability models in the inversion process. As noted above, the relation for Ψ_m requires a reference model (m_0) against which solutions are compared. This can be an actual 2D model constructed from known geology or a estimate of half space conductivity or chargeability. In addition, the modeling process will start from an initial model which has the same general form. In general, an average half space conductivity and chargeability based on the field values is the best model to start from

and this is the default model for both inversions if none other is specified. This will ensure that Ψ_m converges to a value which is not too large. The initial and reference models can be used to estimate the depth of investigation. If two inversions are performed with very different reference models, there will be regions in the final models which will be the same in both inversion and peripheral regions where the final models will resemble the reference models. An example is shown below:

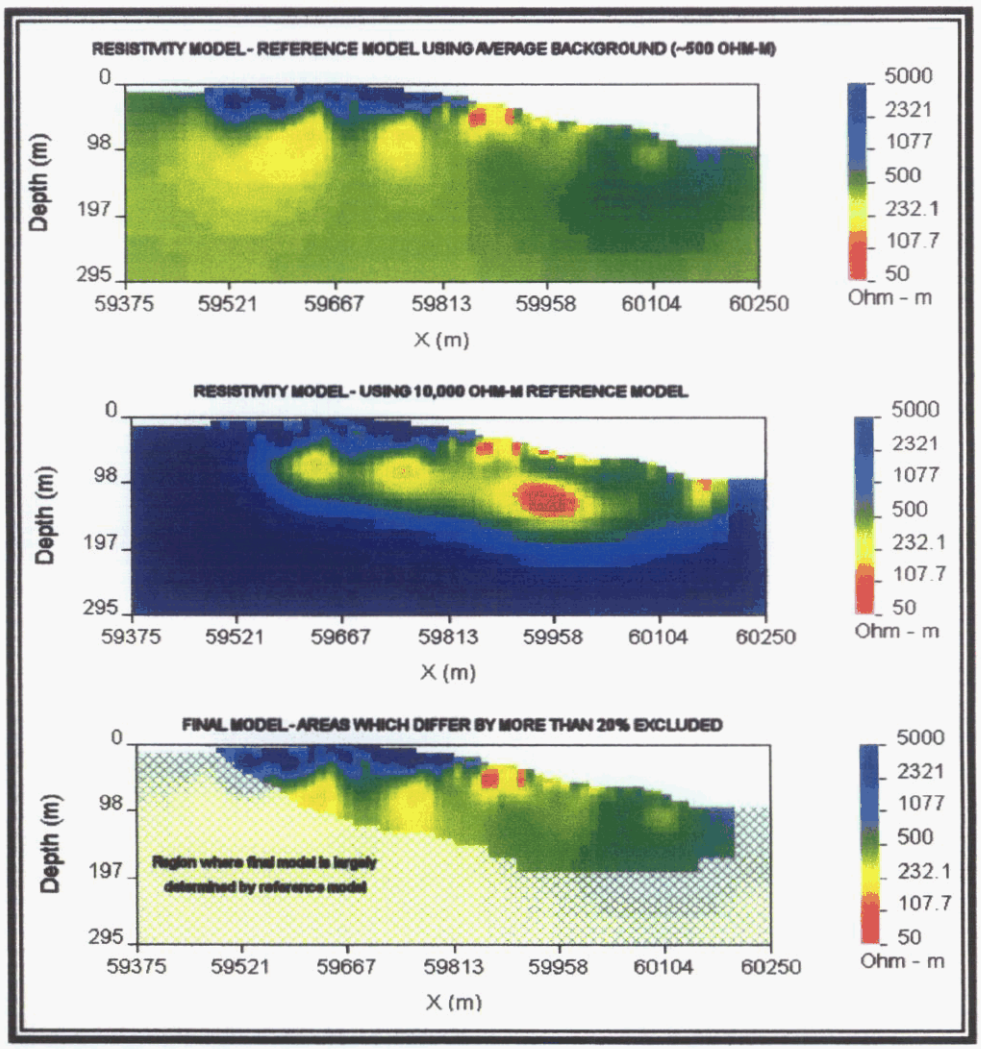

Depth of investigation determined from inversion results using different initial and reference models.

8.0 DATA PROCESSING, INTERPRETATION & PRODUCTS

The following procedures were used to prepare and invert the induced polarization and resistivity data:

1. Data review. The IP data was reviewed and edited prior to preparing pseudosections and preparing the data sets for inversion. Duplicate readings were averaged and duplicates removed from the data base to leave only a single reading at each station and separation. Readings with large errors which did not repeat within 10% were deleted from the data base.

2. Pseudosection plotting. Pseudosections of the apparent resistivity, chargeability and error in chargeability were prepared from the final edited data. The chargeability, error in chargeability and resistivity sections were scaled to the range on each line.

3. Data formatting. The apparent chargeability, resistivity (in normalized V/I) and topographic data were formatted for entry into the UBC inversion program.

4. Resistivity modelling. For each line, errors in the apparent resistance (V/I) were assigned to the data. There is no means of directly quantifying these errors because neither the transmitter nor receiver record the apparent error in the current or voltage. Errors were assumed to be 0.0002 + 2% ohms. Following error assignment, the data was inverted using these error values. The default mesh is quite adequate for the data set because of the low relief along the survey lines. The default initial and reference models are based on an average of the apparent resistivity. After the default run, the data was inverted a second time using initial and reference models which were 10,000 ohm-m (a much higher value than the average 200-500 ohm-m in the survey area). The purpose of this second run was to generate a model with a background resistivity which was greatly different than the average values used in the default run. After the second run, the two models were compared and regions which showed more than 20% discrepancy were blanked out in the final models. In these blanked out regions, the final models are not sensitive to the field data and no reliable subsurface information is likely contained in these portions of the models.

5. Chargeability modelling. For each line, the observed standard deviation in the chargeability was used as a measure of error in the observed apparent chargeability. The IP data was first inverted using default values. The same mesh used in the resistivity modelling and the final DC resistivity model was used in the IP inversion together with default initial and reference chargeability

models. After the first run, the data was inverted a second time using initial and reference models which incorporated background chargeabilities of 100 mV/V (a much higher value than the average 0-10 mV/V in the survey area). The two models were then compared and regions which showed more than 20% discrepancy were blanked out in the final models. In these blanked out regions, the final models are not sensitive to the field data and no reliable subsurface information is likely contained in these portions of the models.

6. *Image extraction.* After the modelling was complete, data ranges were compiled and overall data scales were assigned for both the resistivity and chargeability models. A resistivity scale covering the range from 30 to 5000 ohm-m was used as a standard scale for all resistivity models. A consistent scale of 0 to 50 mV/V was used in the chargeability model sections. Several lines contain small regions with modelled chargeability in excess of the maximum value. Final images were generated with the inversion software and converted to JPEGs without further editing.

7. *3D model generation.* The inversion results for each lines were converted to UTM coordinates and elevation using proprietary software and plotted with Rockworks 3D imaging software.

8. *Digital archive.* The final IP data, digital copies of the pseudosections, inversion images and 3D images were written to CD-ROM.

Final digital data is appended to this report in Excel spread sheet format. Readings with unacceptable errors and which did not repeat have been deleted from this final data set. Also included are GPS position measurements taken along the survey lines. These show the averaged location of the survey point in UTM coordinates, NAD 1983 datum, Zone 7N projection. This data is contained in an ASCII text file (GPS Points.txt).

Pseudosections of the final IP data are appended to this report in the back pockets. These sections were prepared at 1:2500 and show the apparent chargeability, apparent resistivity and error in apparent chargeability in standard pseudosection format. The chargeability, error in chargeability and resistivity sections are scaled to the data ranges within each section.

The inversion results are collated in Appendix D. These images show the observed data, the model generated response for comparison, the 2D resistivity distribution in the final model and the 2D chargeability distribution in the final model. Convergence curves are also shown to assist the reading in assessing the quality of the inversion. In some cases, the final models failed to replicate the high gradients observed in the

chargeability data. In these models, convergence to the target misfit was not achieved.

9.0 GEOLOGICAL SETTING & TARGET RESPONSE

The general geology in the area of the Nikki Property is described by Gordey and Makepeace (1999). The property straddles the east-west striking contact between the Permian Skolai Group and the overlying Dezadeash Group to the south. The regional stratigraphy in the property area is summarized below:

Unit (abbreviation)	Description
Dezadeash Group **(JKD1)**	interbedded light to dark buff-grey lithic greywacke, sandstone, siltstone, thin dark grey shale, argillite, phyllite and conglomerate; rare tuff
Skolai Group **(PS)**	tuff, breccia, argillite, agglomerate, augite-phyric basaltic to andesitic flows (Station Cr. Fm); succeeded by thin-bedded argillite, siltstone, minor greywacke and conglomerate and local thin basaltic flows, breccia and tuff (Hasen Cr. Fm)

In the area of the property, the assemblage is intruded by a Cretaceous (?) granodiorite plug. Figure 3 is a schematic geology map showing the relationship between the grid and the geology mapped during the 2004 exploration season. The following map units are shown in this figure:

Unit	Description
8	Epidote-chlorite-tremolite skarn
6	Dark green to black, fine to medium grained intrusive basaltic dyke rock with horneblende blebs < 2mm.
5	Quartz-feldspar porphyry
4	Granodiorite: altered with limonite and sulphides
3	Granodiorite - unaltered

Unit	Description
2	Diorite with 10-40% hornblende, 55-88% plagioclase, including fine grained variation
1	Meta-chert with minor mudstone (Dezadeash?)

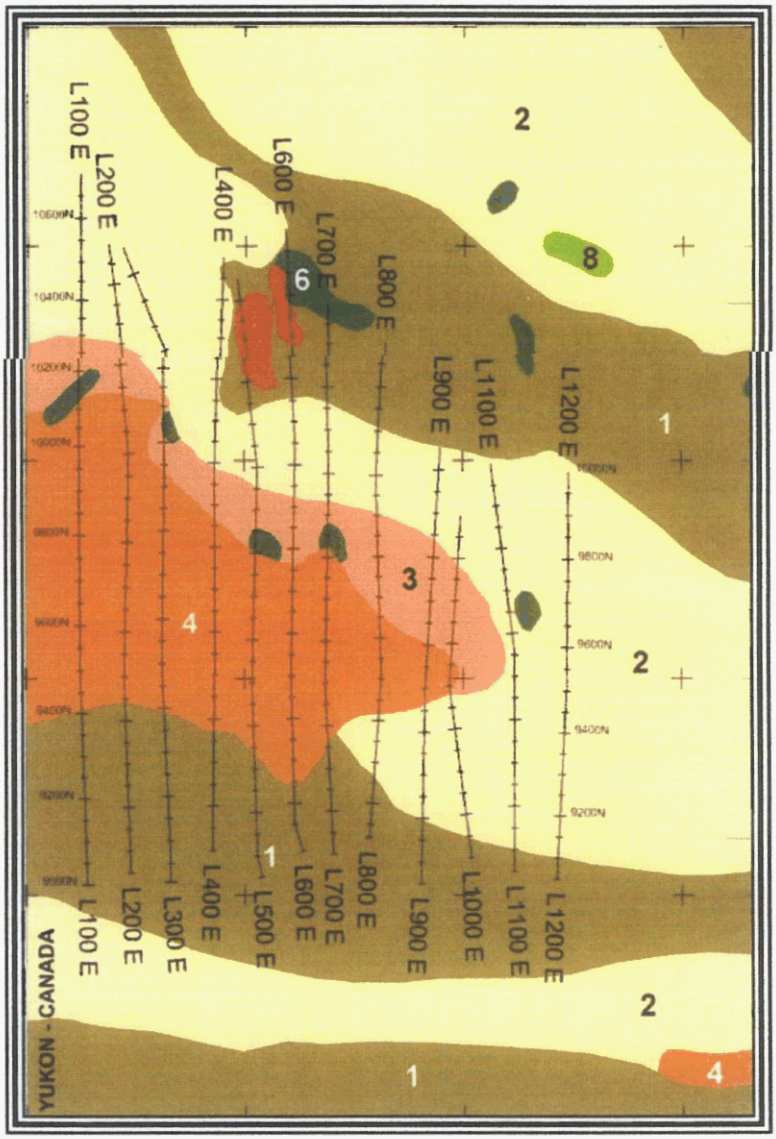

Figure 3. Property geology and IP survey grid.

The Nikki Property covers the Trudi Showing (Minfile 115K82). The property was staked in 1910 and dropped and then restaked by Hector Rail in 1968. The property was subsequently optioned by Pacific Giant Steel Ores Ltd. and later by Canyon City Exploration Ltd. Restaked as the Trudi Claim in the following year by B. Watson, the property was optioned by Quintana Minerals Corporation Ltd. which conducted soil sampling, geological mapping and drilled two holes (952 feet). The property was abandoned thereafter until being restaked by ATAC Resources Ltd. The showing is centred on the granodiorite stock which exhibits pyritic, chloritic and sericitic alteration. Earlier soil sampling outlined a soil copper anomaly 1800 m long by 600 m wide and drilling returned grades of 0.13% copper and 0.005% MoS_2. Soil sampling in 2004 outlined both gold and copper soil geochemical anomalies in and north of the granodiorite stock.

The IP array used in the survey has a maximum depth of penetration for a steeply dipping target in the order of 180 m. Flat lying or wide steeply dipping targets should be detectible to larger depths. Targets less than 25 m wide are difficult to detect with the 50 m dipoles used in the array. Thin (15-25 m) targets would be expected to produce single slash anomalies whose dip in a pseudosection has no bearing on the dip of the source body. Near surface thin tabular sources or small pods may produce dipole or single station anomalies.

A porphyry system with a classic Lowell and Gilbert alteration assemblage would be characterized by base metal sulphide mineralization along the contact between the core potassic alteration zone and the surrounding phyllitic alteration zone. Both copper content and sulphide grades would be higher near the core of the intrusion while higher gold grades would be elevated in the adjacent peripheral areas. In terms of IP response, sulphide mineralization at the contact between potassic and phyllitic alteration zones would generate a chargeability high although the response may be muted if clay alteration significantly lowers the resistivity of the rock. The apparent resistivity of the surrounding clay alteration halo (phyllitic and argillic zones) would be lower than the potassic core of the intrusion. Naturally, the response of given porphyry systems will vary widely depending upon differences in alteration and the presence or absence of structural displacements which may dismember the porphyry deposit.

10.0 RESULTS

The data is of generally good quality in areas where ground contact could be achieved. Some readings at large separations contain high errors but these readings repeated and have been retained despite their high errors. Features consisting of a single high and paired low (dipole response) at any separation are likely caused by small chargeable pods near an electrode. There are also single slash anomalies whose dip

in a pseudosection has no bearing on the dip of the source body. In general, the tops of ridges are more electrically resistive - even at large separations - than surrounding areas; this suggests that these ridges are formed by silicified or unweathered rocks.

In general, the survey detected a large zone of low resistivity less than 200 ohm-m in a background of about 500 to 1000 ohm-m. This central zone of low resistivity is coincident with the mapped altered granodiorite unit but extends further to the east in the subsurface. Surrounding this zone of low resistivity is a zone of high chargeability which, from west to east, wraps around the upper north side of the resistivity low then swings underneath it and finally emerges south of the resistivity low. This zone is defined by a minimum chargeability of 5 mV/V but includes regions of much higher chargeability. In the following discussion, the zone of low resistivity is referred to as the central resistivity low and the large zone of chargeability is referred to as the enveloping chargeability high.

A detailed description of the results for each line follows:

Line 100E

The most significant response on L100E is the central resistivity low which is coincident with the zone of altered granodiorite (9500N to 9900N). On the north margin of this zone is a region of slightly elevated chargeability but this anomaly is not significant in terms of its amplitude. There is a high chargeability anomaly at the end of the line likely caused by a small pod. Chargeabilities are suppressed in the resistive rocks on the ridge tops and at 9500N, this phenomenon is apparent only at short separations and thus appears to be due to weathering rather than lithology. The inversion results suggest the presence of a large deep low resistivity feature (< 200 ohm-m) flanked, on the north side, by a chargeable zone (25 mV/V).

Line 200E

The central resistivity low extends from 9600N to 10000N on Line 200E and is bounded on the north side by a thin high chargeability anomaly at 10050N. There is a chargeability anomaly visible only at large separations centred at 9700N. The resistivity inversion converged well and the model indicates that the lowest resistivity in the central resistivity low is at 9500N. The chargeability model also converged well and positioned a zone of slightly elevated chargeability at 10100N (16 mV/V).

Line 300E

The central resistivity low extends from 9500N to 9850N and is flanked on the north side by a shallow chargeability high. There is a zone of negative chargeability

associated with a thin resistive anomaly at 9200N. The resistivity inversion converged to a target misfit solution while the chargeability inversion was unable to converge to a satisfactory solution, failing only to model the high amplitude chargeability highs at n=6 near 9400N. The chargeability model indicates the continuing presence of the enveloping chargeability high north and above the central resistivity low. The lowest resistivity (30 ohm-m) appears to be near 9450N and may be associated with a thin near surface feature at this location.

Line 400E

The central resistivity low extends from 9300N to 9800N on Line 400E and is flanked by a zone of thin, highly chargeable sources to the north. The chargeability anomalies north of the central resistivity low are unusual. The anomalies are paired, south dipping single slash, high amplitude highs and lows. The negative anomalies are higher amplitude than the positive anomalies indicating that the sources are likely off-line (ie. either east or west of the survey line). It is possible that these anomalies are caused by a zone of en-echelon, highly chargeable, thin (< 25 m) bodies. There is chargeability suppression at n=1 over these anomalies and they likely do not outcrop. Both the resistivity and chargeability anomalies failed to converge to target misfit solutions but the misfit was greatest for the case of the chargeability because of the negative chargeabilities. The UBC-GIF algorithm is unable to model off-line responses and thus cannot deal well with negative chargeabilities. As a result, the chargeability model shows only slightly elevated chargeability in the area of the single slash anomalies. It is more likely that this area contains a series of highly chargeable, thin sources at depths to top in the order of at least 25 m.

Line 500E

Line 500E is an important line in that the enveloping chargeability high wraps around the central resistivity low along this line and highly chargeable features are intimately associated with the zone of low resistivity. The central resistivity high extends from 9250N to 9800N and is most intense at 9600N. There are a series of complex high intensity chargeability highs and lows along the line with chargeabilities suppressed at short separations (n=1 to n=3). High errors are associated with the chargeabilities at larger separations but the data is repeatable. The resistivity inversion failed to converge to the target solution but the chargeability model did converge to a target solution, largely because the reading errors were so high. The resistivity inversion indicates that the central resistivity low may have split on this line at about 9600N while the chargeability inversion suggests that the central resistivity high is underlain or nearly coincident with a zone of elevated chargeability.

Line 600E

The central resistivity low extends from 9400N to 9750N on Line 600E. There is broad zone of elevated chargeability at large separations from 9400N to 9600N; this may underlie the central resistivity low in this interval. To the north and south of this low amplitude anomaly are high amplitude, south dipping single slash anomalies which appear to be caused by thin highly chargeable bodies. Negative high amplitude chargeability anomalies on the south side of the central resistivity low are possibly caused by off-line chargeable bodies either west or east of the survey line. The chargeability anomalies appear to envelope the central resistivity low on its southern boundary. The resistivity inversion converged to a target misfit solution while the chargeability inversion failed to converge to the target misfit solution on account of the high amplitude anomalies and the presence of negative chargeabilities. In particular, the inversion failed to replicate the response on the south end of the survey line. It appears that there is a zone of thin (<25 m) highly chargeable, possibly en-echelon structures in the interval from 9200N to 9450N.

Line 700E

The central resistivity low narrows on this line and extends from 9400N to 9600N. The line does not extend far enough south of this feature to conclusively demonstrate that there is no chargeable material here. To the north of the central resistivity low, several asymmetric, relatively low amplitude chargeability anomalies are associated with a keel-like body of high resistivity rock on a flat bench. The resistivity inversion easily converged to the target misfit and indicates that the central resistivity low is shallowest at its southern end near 9350N. The chargeability model failed to converge to the target misfit and was unable to model the high amplitude readings near 10100N. Nonetheless, the model indicates the continued presence of chargeable material north of the central resistivity low. It appears that this northern zone of chargeability diverges from its position flanking the central resistivity low along this line and may indicate that a separate source of chargeability associated with rocks of higher resistivity is present here.

Line 800E

The central resistivity low continues to narrow along this line and is present from 9450N to 9600N only. At the north end of the line, there is a zone of highly resistive rock (1700 to 5000 ohm-m) near the crest of the ridge. Immediately south and apparently beneath this zone of high resistivity is a region of slightly elevated chargeability north of the central resistivity low. There are no significant chargeability anomalies on this line. The resistivity inversion achieved the target misfit easily but the chargeability inversion failed to reach the target misfit because of complexity at large separations at the south end of the line. It appears that both the chargeability and resistivity anomalies are strongly tapered along this line.

Line 900E

On Line 900E, the central resistivity low bifurcates into pair of weak lows covering the interval from 9500N to 9600N. There are a number of single slash and dipole chargeability anomalies on this line, the most intense of which is a complex high at n=3 to 6 centred at 9600N. As on lines to the west, both positive and negative chargeability anomalies are present. The resistivity inversion suggested that the central resistivity low has plunged to a depth of 100 to 150 m below surface while the rather poor chargeability inversion suggests only the presence of a deep chargeability source north of the central resistivity low. The inversion model failed to replicate the chargeability high at 9600N but did indicate a zone of elevated chargeability here.

Line 1000E

The central resistivity low is visible on L1000E in the interval from 9300N to 9450N. A flat bench from 9600N to 9800N is underlain by highly resistive rock. High chargeabilities at n=5 and n=6 paired with lows at shorter separations were recorded in the interval from 9300N to 9700N. Both the resistivity and chargeability models failed to converge to the target misfit solutions with the greatest misfit occurring in the chargeability modelling at large separations. The resistivity model suggests that the central resistivity low continues to plunge to the east and that it may be underlain by a large zone of chargeable material. Both the resistivity and chargeability models suggest that thin, perhaps pod-like structures are present over the central resistivity low.

Line 1100E

Poor contact and high errors prevented recording some data on the north end of Line 1100E. The remains of the central resistivity low are visible at separations greater than n=3 from 9200N to 9300N. Two single slash chargeability anomalies are associated with the resistivity low and there are a number of other small complex anomalies to the north. The resistivity inversion inconclusively suggests that the axis of the central resistivity low is at 9200N while the chargeability inversion only suggests the presence of small pods of chargeable material along the line.

Line 1200E

The central resistivity low is present in the interval from 9200N to 9400N on this line, even at short separations. This sudden change in elevation and width of the central resistivity low may indicate fault offset between Lines 1100E and 1200E. High chargeability anomalies at large separations are present along the length of the line and two asymmetric highs are present at 9550N and 9750N. There is a keel-like body

of high resistivity coincident with a small plateau, suggesting that this is underlain by a separate thin resistive rock unit.

Discussion

The inversion models of resistivity and chargeability were contoured in three dimensions to produce block models of these properties in the subsurface. The 3D models were generated by contouring the physical properties using an anisotropic gridding algorithm weighting the contribution of nearby points by their distance r from the sample point. Nearby points were weighted as $1/r^3$ horizontally and as $1/r^4$ vertically. This forced the model to retain the vertical complexity of the original models. The resistivity model was then constructed by drawing an isosurface enclosing all material with resistivity less than 200 ohm-m (conductivity greater than 5 mS). Similarly, the chargeability model was constructed by drawing an isosurface enclosing all material with chargeability greater than 5.0 mV/V. These values were selected to generate surfaces which extended from line to line, which had some relation to the known geology but which did not include numerous spurious spot anomalies generated when the isosurface contouring threshold is set near the background value. In the models, the chargeability isosurface enclosing all material with chargeability greater than 5 mV/V is green while the isosurface enclosing all material with resistivity less than 200 ohm-m is coloured light blue. The data is displayed in isometric views with coordinates in NAD83 UTM coordinates along the X and Y axis. The vertical axis is elevation in metres above mean sea level. The squares shown in the reference grids along each axis are 100 m on a side.

Figure 4 is a view of the 3D model from the southeast showing the shaded surface topography (grey) and the two isosurfaces. The blue resistivity isosurface forms a rod or sausage-shaped body central resistivity low plunging to the east across the survey grid. On the west end of the model, the resistivity low outcrops but it plunges to a depth of 150 m or more on the east end of the grid except for a small shallow on the last line in the southeastern corner. The central resistivity low may be fault offset with apparent uplift to the east between Lines 1100E and 1200E. Peripheral to the central resistivity low is an enveloping chargeability high shown in green. This feature is north of the central resistivity low in the western portion of the model but it passes beneath the eastern end of the low and reappears on the south side of the central resistivity low at its eastern end.

Figure 5 is a top view of the 3D model showing the mapped geology and the two isosurfaces. The contact between the altered granodiorite in the main intrusive body near the Alaska-Yukon border and all other rock units is shown in red (Unit 4). The central resistivity low in blue and the enveloping chargeability high in green are shown beneath the surface geology which is draped on shaded topography. It is readily

apparent that the central resistivity low is coincident with the exposed altered granodiorite. Consequently, it appears that this resistivity low maps the extension of this rock unit to the east beneath cover rock. This could be confirmed by examining the rocks at the southern end of L1200E where the resistivity low appears to resurface. The enveloping chargeability high has a complex geometry which appears to be related to the location of the metasedimentary rocks. With the exception of where the enveloping chargeability high passes beneath the resistivity low, the chargeability high tends to remain solely within the metasedimentary rock unit (Unit 1).

Figures 6 and 7 are top views of the 3D model showing the two isosurfaces with overlying copper and gold geochemistry respectively. In Figure 6, it is apparent that the main copper soil geochemical response closely follows the central resistivity low although a weaker subsidiary response trends northwest along the enveloping chargeability high to the north. The response in gold is peripheral to the central resistivity low and the altered granodiorite, apparently following a northwest trend of topography and chargeability.

It is noteworthy that there appears to be a northwesterly grain to both the geophysical and geochemical responses. Both the soil geochemical responses follow a northwest trending spur north of the altered granodiorite. Similarly, the enveloping chargeability high appears to wrap beneath the central resistivity low along a NNW trending axis. Structures with a similar orientation are considered important in the adjacent districts of Alaska (eg. Pogo, Uncle Sam, etc.)

The limited geological information available to the author combined with the results of the geophysical survey suggest that mineralization on the Nikki Property appears to be more affiliated with skarn rather than true porphyry style mineralization. The resistivity signature does not suggest that there is a large envelope of clay (phyllic or argillic) alteration surrounding the intrusion. The core of the intrusion does not appear to have undergone potassic alteration; quite the contrary, rather than being resistive the intrusion is the lowest resistivity feature on the geophysical grid. Finally, while there is an enveloping chargeability high which could be shoe-horned into a porphyry model, this zone is rather errant. It tends to follow reactive rock units adjacent to the intrusion and, perhaps, follows a structure cross-cutting the intrusion. Since these two styles of mineralization form a continuum, further exploration might be guided by a strategy which continues to investigate both possibilities.

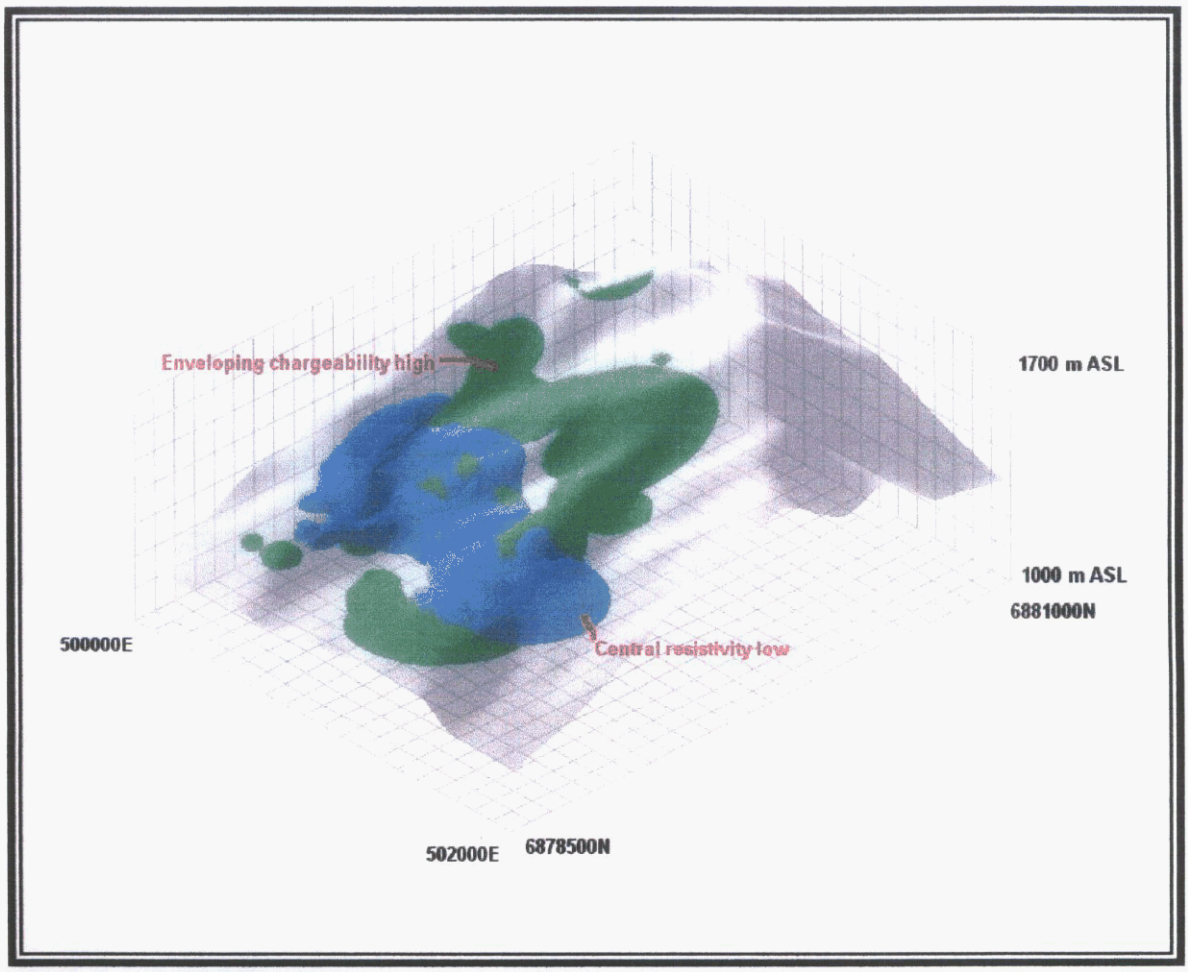

Figure 4. Isometric view of a 3D model of the chargeability (green > 5 mV/V) and resistivity (blue < 200 ohm-m). Surface topography is shown as shaded grey. The central resistivity low plunges from west to east and is coincident with altered granodiorite on the west end of the grid. The enveloping chargeability high is above and north of the central resistivity low except on the east end of the low where it wraps beneath it.

Figure 5. Top view of 3D model showing central resistivity low (blue) and enveloping chargeability high (green). Mapped contact of the altered granodiorite (Unit 4) is shown in red. The central resistivity low plunges to the east. Chargeability anomalies comprising the enveloping chargeability high are developed in both the metasediments (Unit 1) and diorite (Unit2) surrounding the granodiorite intrusion.

Figure 6. Plan map of copper soil geochemical survey results (red > 1000 ppm, orange > 500 ppm) overlain on shaded topography. Central resistivity low (blue) and enveloping chargeability high (green) are visible beneath. Each square is 100 m x 100 m.

Figure 7. Plan map of gold soil geochemical survey results (red > 200 ppb, orange > 100 ppb) overlain on shaded topography. Central resistivity low (blue) and enveloping chargeability high (green) are visible beneath. Each square is 100 m x 100 m.

11.0 CONCLUSIONS

The results of the induced polarization / resistivity survey at the Nikki Property support the following conclusions:

a. There is a 100 to 500 m wide zone of low resistivity defined by material less than 200 ohm-m in a background of 500 to 1000 ohm-m. This zone follows the mapped trace of altered and mineralized granodiorite extending from the Alaska border east across the geophysical grid. It plunges to the east along strike although there appears to be some uplift and widening at the eastern end of the grid.

b. There is a zone of elevated chargeability defined by a surface enclosing material with chargeability in excess of 5 mV/V in a background of 1-2 mV/V. Within this zone are regions with intrinsic chargeability in excess of 40 mV/V. This enveloping chargeability high follows the north side of the central resistivity low in the west and passes beneath it on the eastern end of the grid.

c. The enveloping chargeability high is clearly associated with the granodiorite intrusion but has developed in the surrounding rocks with the best expression found in metasedimentary rocks. Where it passes beneath the central resistivity low, follows a northwest trend which is also apparent in the geochemical results and may be structural.

d. To date, no geophysical evidence of extensive peripheral clay alteration or central potassic alteration is recorded. Surrounding rocks are quite resistive - especially north of the altered granodiorite and the Unit 4 granodiorite has a low resistivity suggesting it has not undergone potassic alteration.

e. There are numerous high amplitude positive and negative chargeability responses consisting of asymmetric, single slash and dipole anomalies. They are not well modeled in the chargeability inversions which cannot accommodate the high gradients, lack of a full form anomaly and the presence of strong negative chargeabilities. The presence of these anomalies suggests that thin, tabular to pod-like bodies of short strike length are present. In each case, these targets have widths less than 25 m and consequently cannot produce full form anomalies. Many appear at n=1 to n=2 and are thus relatively shallow.

12.0 RECOMMENDATIONS

The following recommendations are made based on the conclusions of this work:

a. Detailed soil geochemistry, trenching and prospecting should be conducted in areas of coincident gold or copper geochemistry and elevated chargeability in the northwest corner of the grid.

b. The results of the geophysical survey should be assessed together with the geological observations to determine an appropriate target model which best fits the geological, geochemical and geophysical data.

c. If additional work is focused on skarn mineralization, total magnetic field and IP surveys should be conducted in conjunction with detailed soil geochemical surveys over prospective flanking reactive horizons. In addition, subsidiary grids may have to be installed to investigate mineralization on NW trending structures cutting the predominantly east-west trending reactive stratigraphy.

d. If additional work is focused on porphyry mineralization, total magnetic field and IP surveys should be conducted over an extension of the present grid to the east.

Respectfully submitted
AURORA GEOSCIENCES LTD.

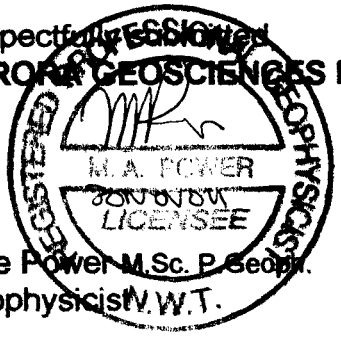

Mike Power M.Sc. P.Geoph.
Geophysicist, Y.W.T.

REFERENCES

Coggon, J.H. (1973). A comparison of IP electrode arrays. Geophysics Vol. 38, No 4. pp 737-761.

Gordey, S.P. and A.J. Makepeace (1999) Yukon Digital Geology, Open File D3826. Geological Survey of Canada: CD-ROM.

Hanneson, J.E. (1990) A model for interpreting IP/resistivity data from areas of steep dip and thin overburden. in: Fink, J.B. *et. al.* (ed.) Induced polarization: applications and case histories. Tulsa: Society of Exploration Geophysicists.

Hohmann, G.W. (1990) Three-dimensional IP models. in: Fink, J.B. *et. al.* (ed.) Induced polarization: applications and case histories. Tulsa: Society of Exploration Geophysicists.

Johnson, I.M. (1990) Spectral IP parameters derived from time domain measurements. in: Fink, J.B. *et. al.* (ed.) Induced polarization: applications and case histories. Tulsa: Society of Exploration Geophysicists.

Oldenburg, D.W. and Y. Li (1994) Inversion of induced polarization data. Geophysics Vol. 59. No. 9. pp. 1327-1341.

Sumner, J.S. (1976) Principles of Induced Polarization for Geophysical Exploration. New York: Elsevier.

Telford, W.M., L.P. Geldart and R.E. Sheriff (1990) Applied Geophysics (2nd Edition) New York: Cambridge University Press.

APPENDIX A. CERTIFICATE

I, Michael Allan Power, M.Sc. P.Geo., P.Geoph., with business and residence addresses in Whitehorse, Yukon Territory do hereby certify that:

1. I am a member of the Association of Professional Engineers and Geoscientists of British Columbia (registration number 21131) and a professional geophysicist registered by the Northwest Territories Association of Professional Engineers, Geologists and Geophysicists (licensee L942).

2. I am a graduate of the University of Alberta with a B.Sc. (Honours) degree in Geology obtained in 1986 and a Masters Degree in Geophysics obtained in 1988.

3. I have been actively involved in mineral exploration the Northern Cordillera since 1988.

4. I have no interest, direct or indirect, nor do I hope to receive any interest, direct or indirect, in ATAC Resources Ltd. or any of its properties.

Dated this 30th day of November 2004 in Whitehorse, Yukon.

Respectfully Submitted,

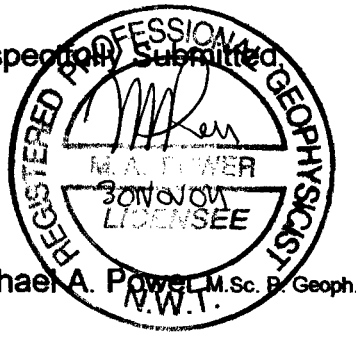

Michael A. Power, M.Sc. P.Geoph. P.Geo.

APPENDIX B. SURVEY LOG

AURORA GEOSCIENCES LTD.

JOB ATAC-04-001-YT
ATAC RESOURCES LTD.
NIKKI IP SURVEY

Period: August 24th - September 7th , 2004

Personnel:

Georges Belcourt	Crew Chief
Josh Melnyk	Helper
Dan Shorty	Helper
Tyson Bourgard	Helper

Tue 24 Aug 04 Mobe
Drive to White River Lodge, leave town at 6:30, arrive at 11:30am. Trans North helicopters slung gear and flew personnel to Nikki campsite. Proceed to setup camp and prep gear for work tomorrow. All is good. Wx: Smoky throughout the day, cooling off in evening. +18C.

Wed 25 Aug 04 Survey
Josh has pain in his knees, will take Tx for a few days. All went well, set up and started reading by 1:50pm. Steep spots but not too bad otherwise. Wx: Rain 1overnight, smoky +15C.

Production: 750m

Thu 26 Aug 04 Survey
Good day, finish line 100 and start line 200. 3.5 hour cross over this aft. Lines will get shorter as we go. Wx: Rain overnight, sunny, smoky a cool breeze, +13C.

Production: 1,250m

Fri 27 Aug 04 Survey
Another good day. Survey to end of line 200, move and setup for line 300. Last few stations along line 200 were shifted to the west approx 30m. The line was missing some pickets in the middle. Wx: Sunshine, warm late day

sprinkles. +18C.

Production: 1,150m

Sat 28 Aug 04 Survey
Survey all of line 300, move and partial setup on line 400. Last few stations along line 300 were shifted to the west on the steep talus slope. Josh unable to continue in field, due to concerns with his knees. Do not want to risk an injury so he will stay on Tx duty. Wx: Sunshine with showers starting at 4:00pm. +15C.

Production: 1,450m

Sun 29 Aug 04 Survey
Setup on line 400, problems with one of the speedy winders delays our start to the day. Survey all of line 400, move all cables to line 500. Steep talus at the north end slows the survey at the end of the day. Wx: Rain overnight, clouds and fog all day, clearing at 5pm. +9C.

Production: 1,400m

Mon 30Aug 04 Survey
Finish setup on line 500, read line, move to 600. Very high errors on most channels causes concern. Many repeats taken, max currents, etc. Many negative M values and inverted decay curves. Wx: Frost overnight, clouds clearing later in the day. +10C.

Production: 1,400m

Tue 31 Aug 04 Survey
Finish setup on line 600, read line, move to line 700. Added electrodes to current setup today, made sure good contacts and more power into the ground. Errors lower, still some negative M values near the chargeability high. 300+ vertical meters on the line. Wx: Sunny, warm & smoky. +14C.

Production: 1,450m

Wed 1 Sep04 Survey
Finish setup on line 700, with some minor problems, read line, move gear to line 800. Inifinity (pseudo) was very close to the creek in a very nice spot, so currents were very much higher today. No problems with the data today. 370+ vertical meter along the line today. Wx: Sunny and windy, less smoke, good views from the top of the mtn. +10C.

Production: 1,300m

Thu 2 Sep 04 Survey
Read line 800 and move all gear to line 900. weather turning, although a good day, more sheep spotted on the mountain today. Current man had some problems reeling in the wire at the end of the day, will position better tomorrow so we can help as well. Wx: overcast, cooling +9C.

Production: 1,200m

Fri 3 Sep04 Survey
Snow all day. Proceed to line 900, read and move cables to line 1000. Inifinite still in swampy area to the south, provides good contacts and currents through the day. Very steep slope at the end of the line with possible 50m missing according to the previous pickets. Wx: colder, rain all night and snow all day, very wet. +4C.

Production: 1,000m

Sat 4 Sep 04 Survey
Snow all night (2inches by morning) very cold to start. Setup on line 1000, very slippery and dangerous in the snow covered talus. Sun starts to shine by 12 noon, warms the day & melts some snow. Finish line 1000 on steep slope at 10+700N not wanting to travel any further up the talus today. Pack up and stach gear on line 1100. Wx: cold to start, warming, overcast. 0C.

Production: 800m

Sun 5 Sep 04 Survey
Cold and clear overnight, heavy frost. Setup on line 1100, steep sections near the top were frozen and thus fairly difficult to traverse. Missed one station in total. Finish early and move gear to line 1200 for tomorrow. Will move a large spooler down the creek to assist winding up wire after surveying complete. Tyson is on day six tobacco-free and feeling great! Wx: Sunny and warm today, clear, good views. +3C.

Production: 950m

Mon 6 Sep 04 Survey
Cold overnight, sunny today. Finish last line, line 1200. Pack cables and rods back to camp, wind up current and infinity wires back to camp and creek. All spools and wire back in camp by 4:30pm. Packing up this evening to be ready for the chopper in the morning. Wx: Sunny and windy on top of the mountain. +7C.

Production: 950m

Tue 7 Sep 04 Demobe

Heli arrives at 9am to demobe to the White River Lodge. Back in two internal and three external net loads. Pack truck and drive back to Whitehorse, arriving at 6pm. No room in truck for any empty drums. Wx: Clear and cool, great slinging weather. +8C.

Survey Days:	13 days
Mobe/Demobe:	2 days
Total IP Production:	15,050m

APPENDIX C. INSTRUMENT SPECIFICATIONS

ANNEX 7: SPECIFICATIONS

Technical:

- Input impedance: 10 Mohm
- Input overvoltage protection up to 1000V
- Automatic SP bucking with linear drift correction
- Internal calibration generator for a true calibration on request of the operator
- Internal memory: 3200 dipoles reading
- Automatic synchronization and re-synchronization process on primary voltages signals whenever needed
- Proprietary intelligent stacking process rejecting strong non-linear SP drifts
- Common mode rejection: more than 100 dB (for Rs = 0)
- Self potential (Sp) : range: -15V - +15V
  : resolution: 0.1 mV
- Ground resistance measurement range: 0.1 - 100 kohms
- Primary voltage : range: 10µV - 15V
  : resolution: 1µV
  : accuracy: typ. 0.3%
- Chargeability : resolution: 10µV/V
  : accuracy: typ. 0.6%

General:

- Dimensions: 31x21x25 cm
- Weight (with the internal battery): 9 kg
- Operating temperature range: -30°C - 70°C
- Case in fiber-glass for resisting to field shocks and vibrations

Instrumentation GDD

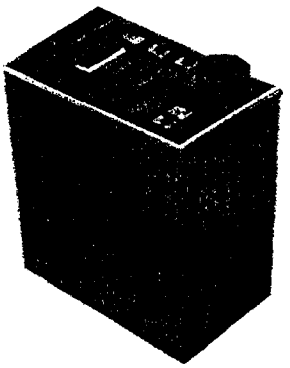

The Induced Polarization Transmitter

TxII-1800 and TxII-3600 Models

For Fast, High-Quality Induced Polarization Surveys in All Field Conditions

Flyers high / low resolution TxII/1 (63 KB) / TxII/2 (1 MB)

At Last, a High-Quality Affordable IP Transmitter

TxII-1800 Model, 1800 watts

Its high power, up to 10 amperes, combined with its light weight and a 21 kg/2000W Honda generator makes it particularly suitable for dipole-dipole Induced Polarization surveys.

Features

- **Protection against short circuits even at zero (0) ohms**
- **Output voltage range: 150 V to 2400 V / 14 steps**
- **Power source: 120 V, Optional: 220 V / 50/60 Hz**
- **Operates from a light backpackable standard 120 V generator**
- **Up to three years warranty**

This backpackable 1800 watts induced polarization (I.P.) transmitter works from a standard 120 V source and is well adapted to

CONTENTS

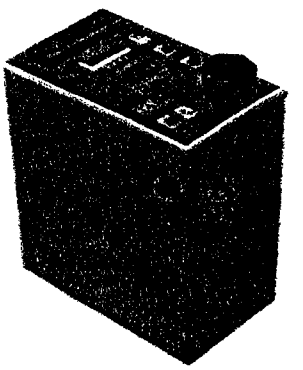

rocky environments where a high output voltage of up to 2400 V is needed. Moreover, in highly conductive overburden, at 150 V, the highly efficient TxII-1800 watts transmitter is able to send a current of up to 10 amperes. By using this I.P. transmitter, you obtain fast and high-quality I.P. readings even in the most difficult conditions.

TxII-3600 Model, 3600 watts

Its high power, up to 10 amperes, combined with a Honda generator makes it particularly suitable for pole-dipole Induced Polarization surveys.

Features

- **Protection against short circuits even at zero (0) ohms**
- **Output voltage range: 150 V to 2400 V / 14 steps**
- **Power source: 220 V, 50/60 Hz**
- **Operates from a standard 220 V generator**
- **Up to three years warranty**

This 3600 watts induced polarization (I.P.) transmitter works from a standard 220 V source and is well adapted to rocky environments where a high output voltage of up to 2400 V is needed. Moreover, in highly conductive overburden, at 150 V, the highly efficient TxII-3600 watts transmitter is able to send a current of up to 10 amperes. By using this I.P. transmitter, you obtain fast and high-quality I.P. readings even in the most difficult conditions.

Specifications

General	
Size TxII-1800	21 x 34 x 39 cm
Size TxII-3600	21 x 34 x 50 cm
Weight TxII-1800	approx. 20 kg
Weight TxII-3600	approx. 35 kg

Operating temperature	-40°C to 65°C
Electrical	
Used for time-domain IP	2 sec. ON 2 sec. OFF
Time Base	1-2-4-8 sec.
Output current range	0.005 to 10 A
Output voltage range	150 to 2400 V
Power source TxII-1800	Recommended motor/generator set: Standard 120 V / 60 Hz backpackable Honda generator Suggested Models: EU1000iC, 1000 W, 13.5 kg. or EU2000iC, 2000 W, 21.0 kg.
Power Source TxII-3600	Recommended motor/generator set: Standard 220 V, 50/60 Hz Honda generator Suggested Models: EM3500XK1C, 3500 W, 62 kg or EM5000XK1C, 5000 W, 77 kg
Controls	
Power	ON/OFF
Output voltage range switch	150 V, 180 V, 350 V, 420 V, 500 V, 600 V, 700 V, 840 V, 1000 V, 1200 V, 1400 V, 1680 V, 2000 V, 2400 V
Displays	
Output current LCD	reads to ±0,001 A
Very cold weather	standard LCD heater on readout
Protection	Total protection against short circuits even at zero (0) ohms
Indicator lamps **(in case of overload)**	- High voltage ON-OFF - Output overcurrent - Generator over or undervoltage - Overheating - Logic failure - Open loop protection

Purchase and Rental Info

Interested by the TxII-1800 W IP or the TxII-3600 W IP transmitter?

It is simple. You can rent it or purchase it. The choice is yours. Here is some information you

APPENDIX D. INVERSIONS

LINE 100E - RESISTIVITY

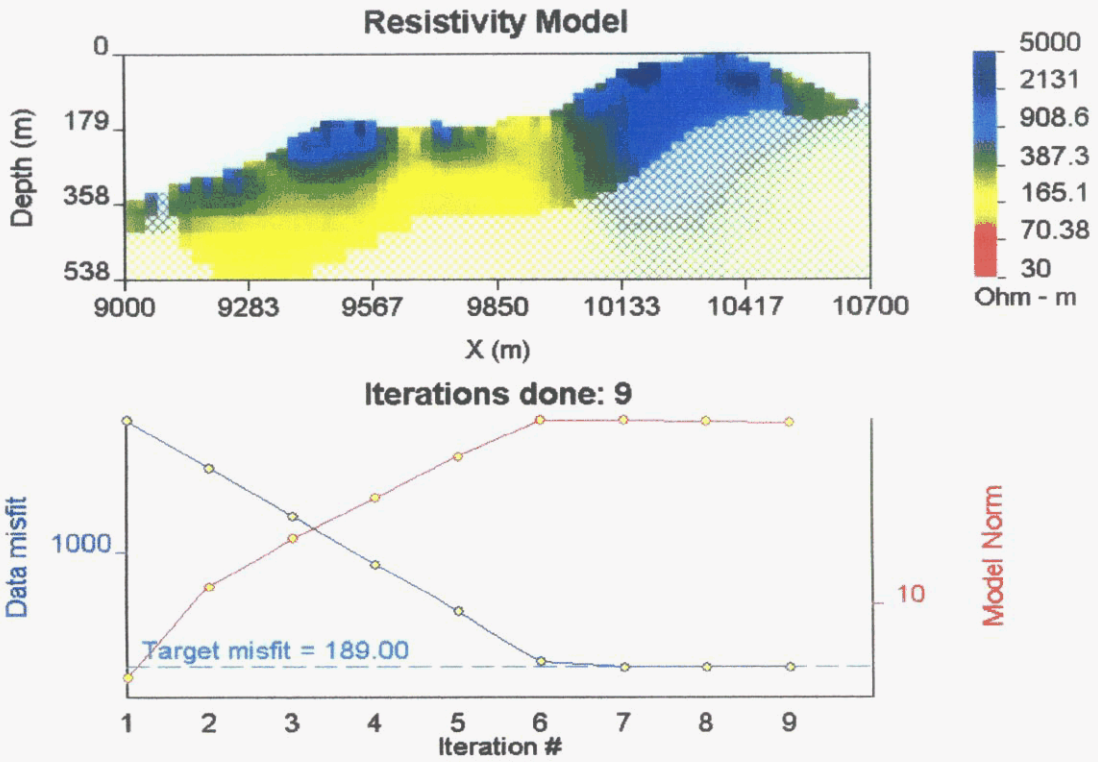

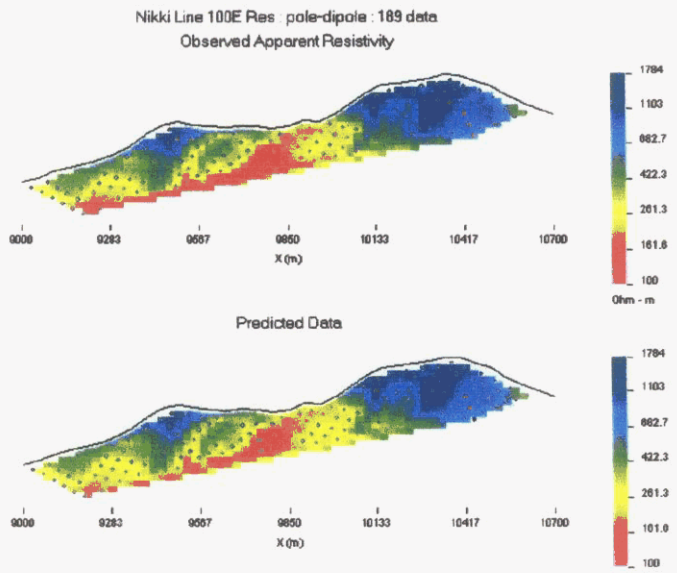

LINE 100E - CHARGEABILITY

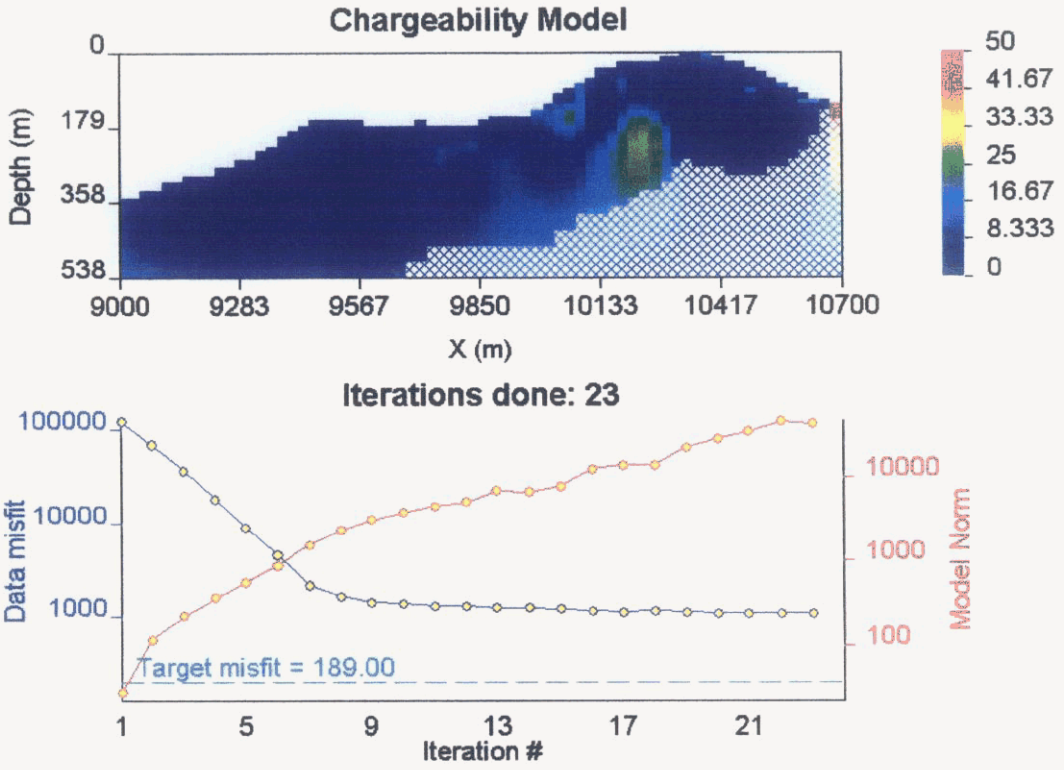

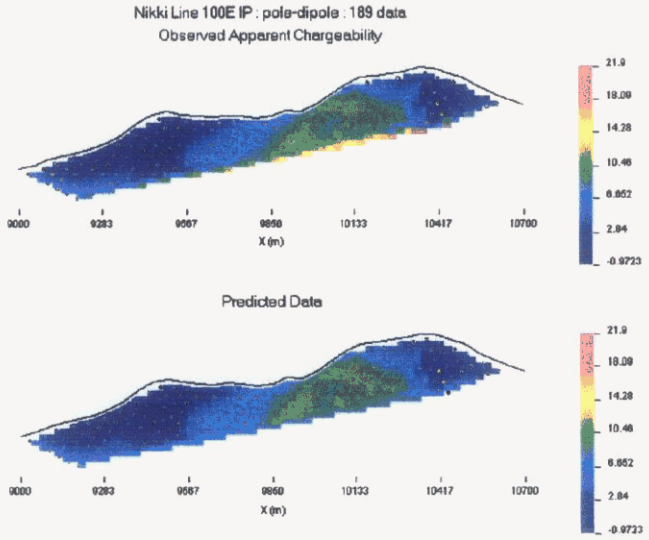

LINE 200E - RESISTIVITY

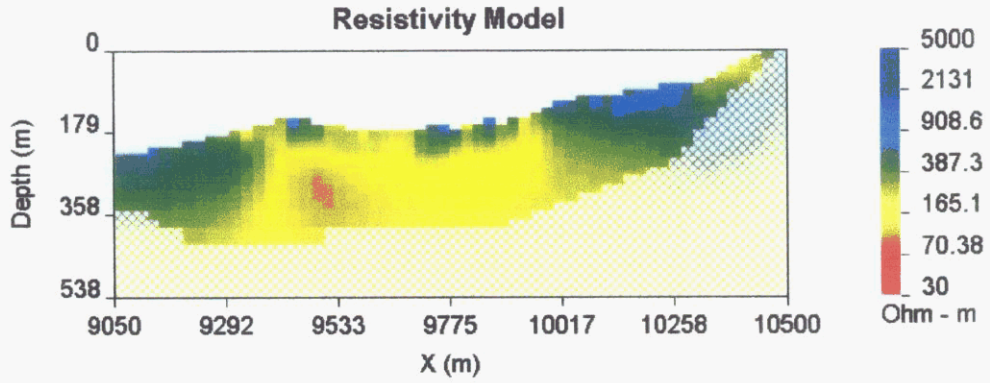

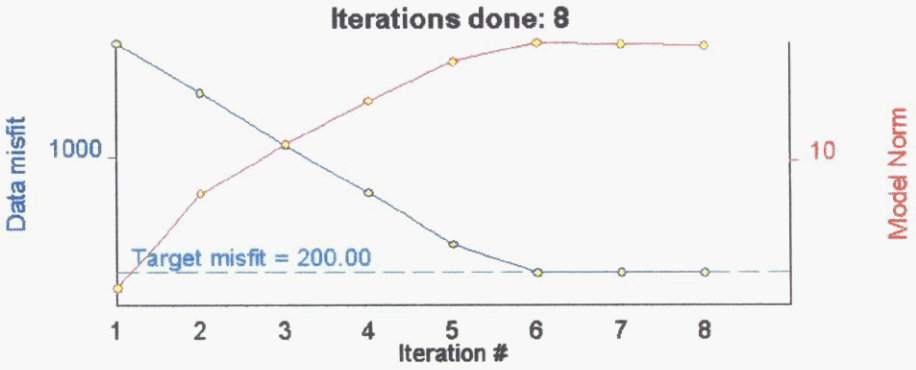

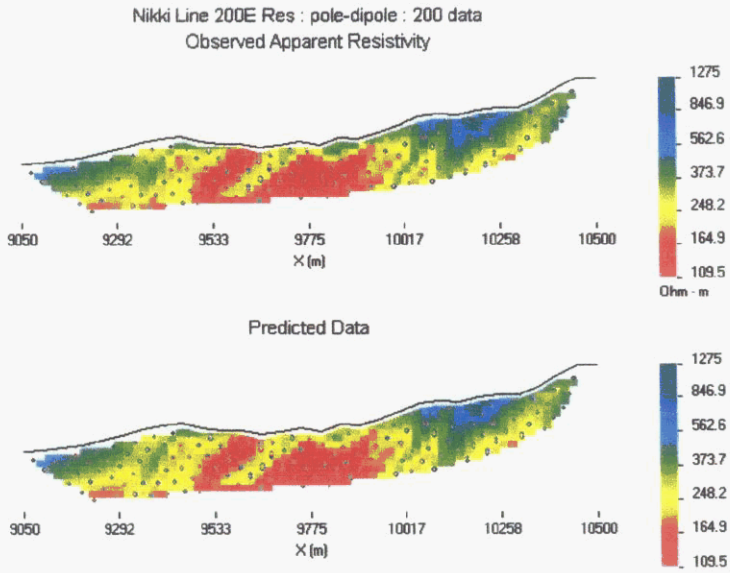

LINE 200E - CHARGEABILITY

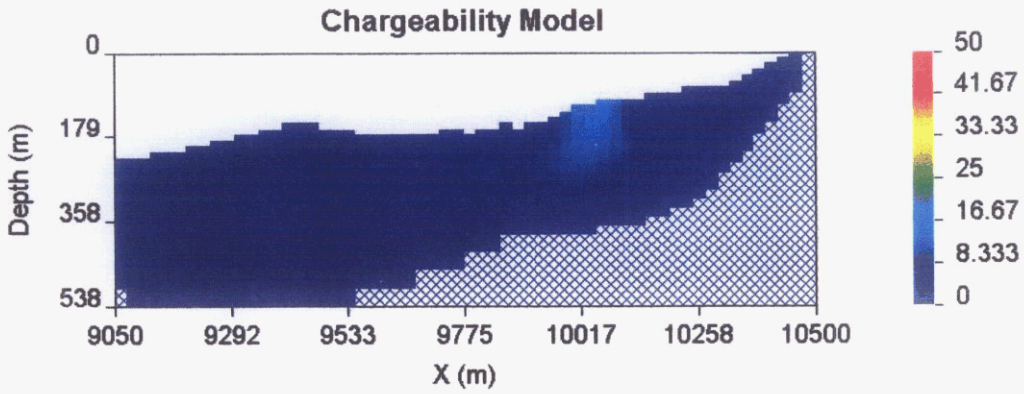

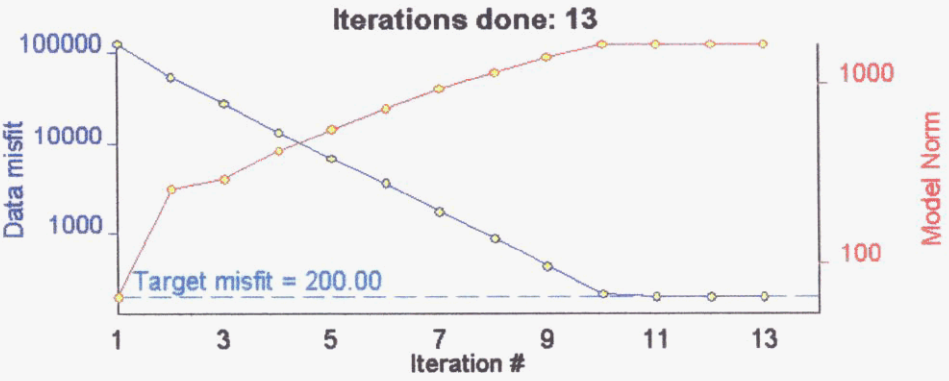

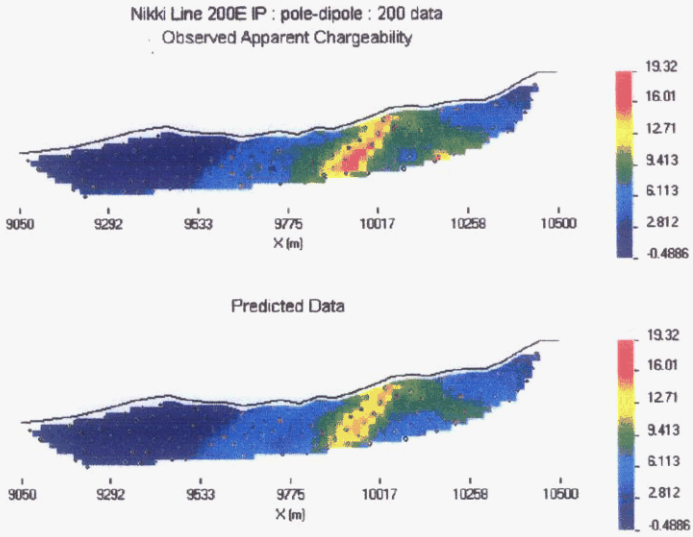

LINE 300E - RESISTIVITY

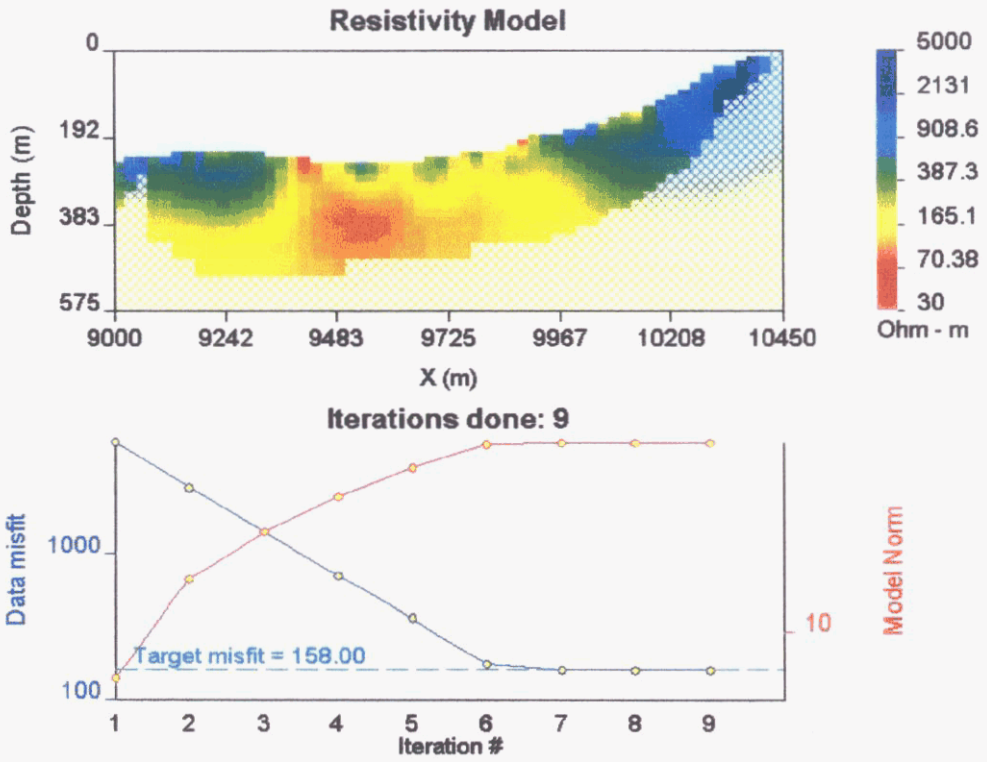

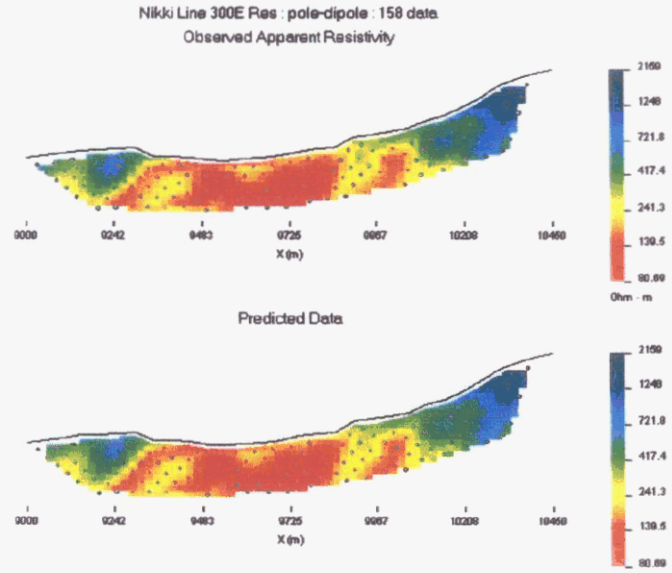

LINE 300E - CHARGEABILITY

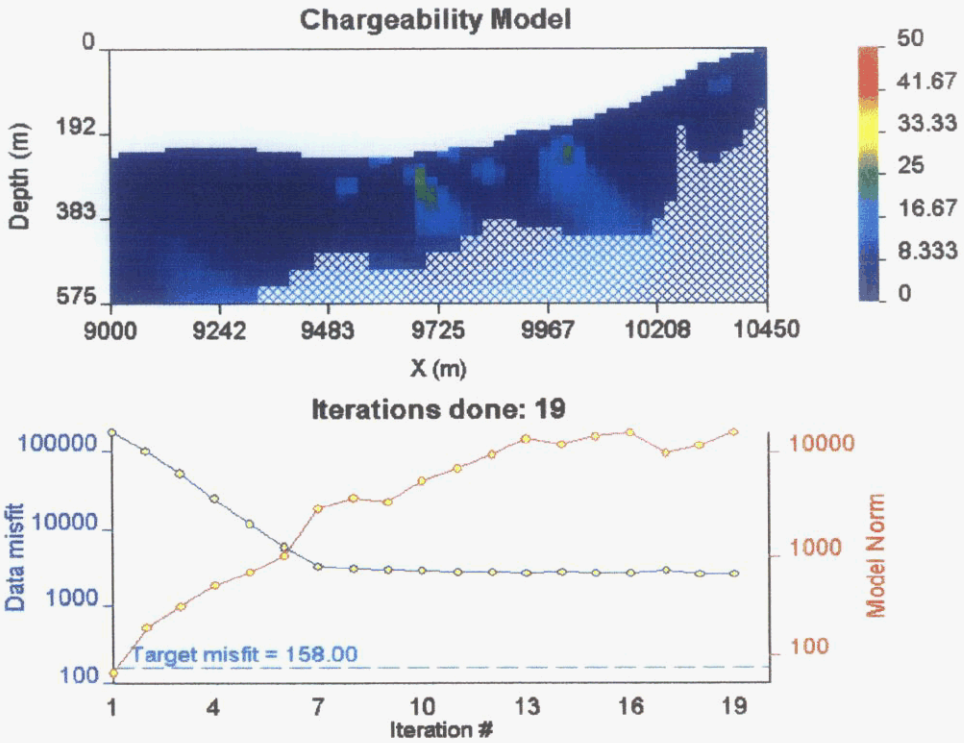

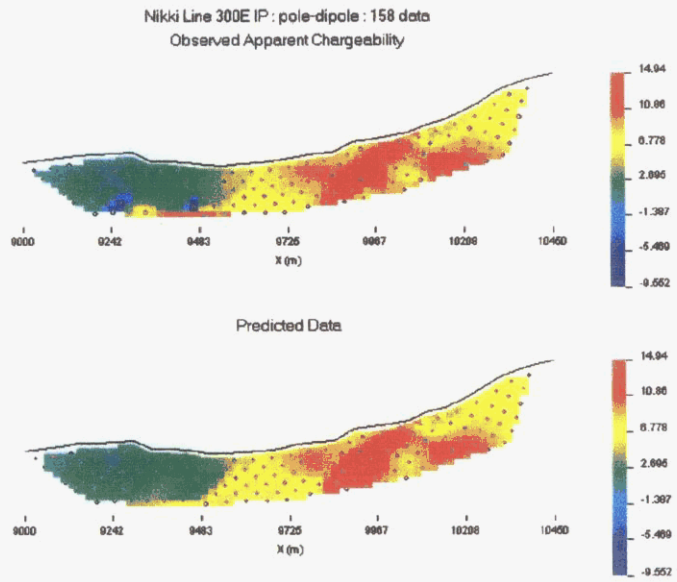

LINE 400E - RESISTIVITY

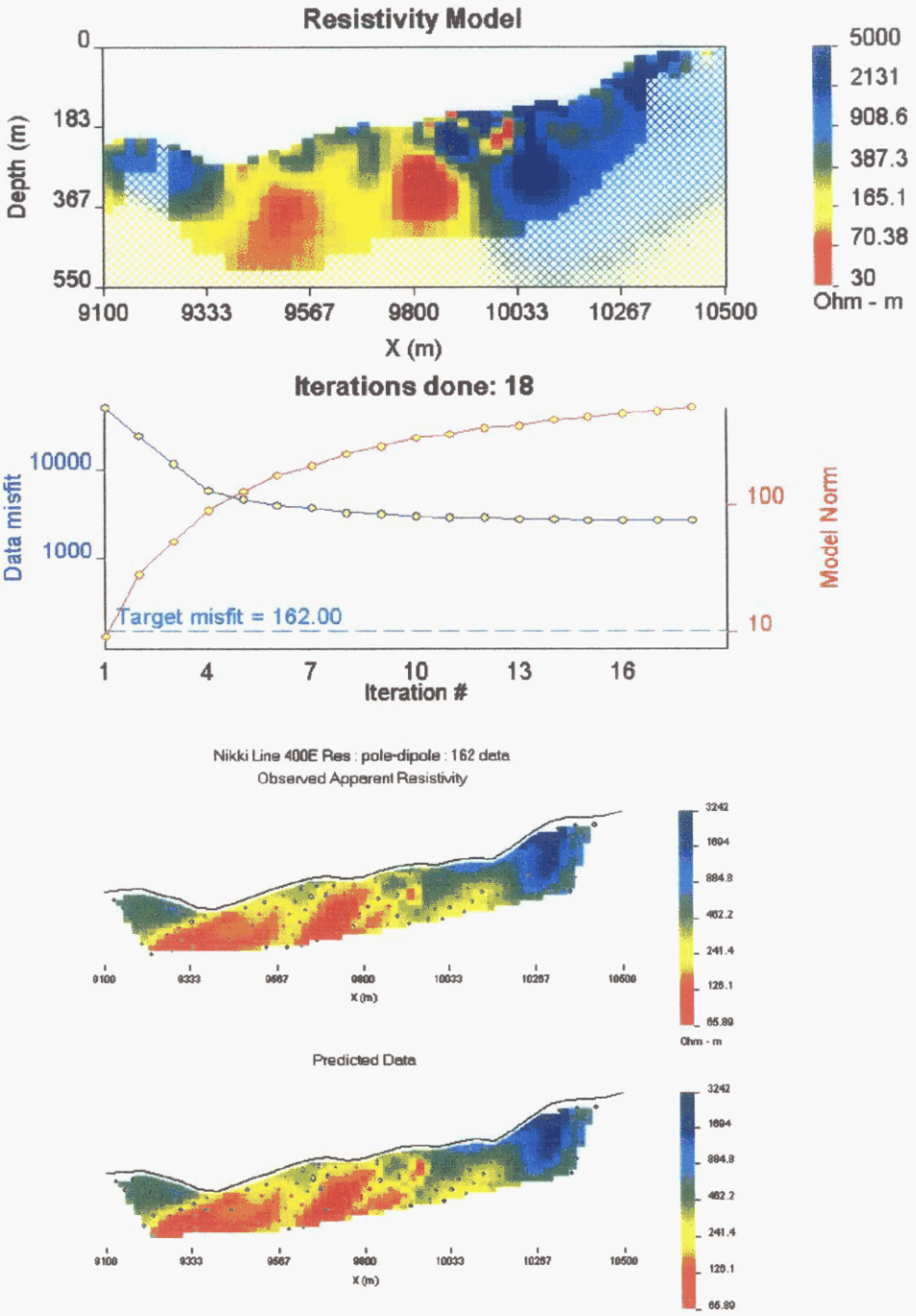

LINE 400E - CHARGEABILITY

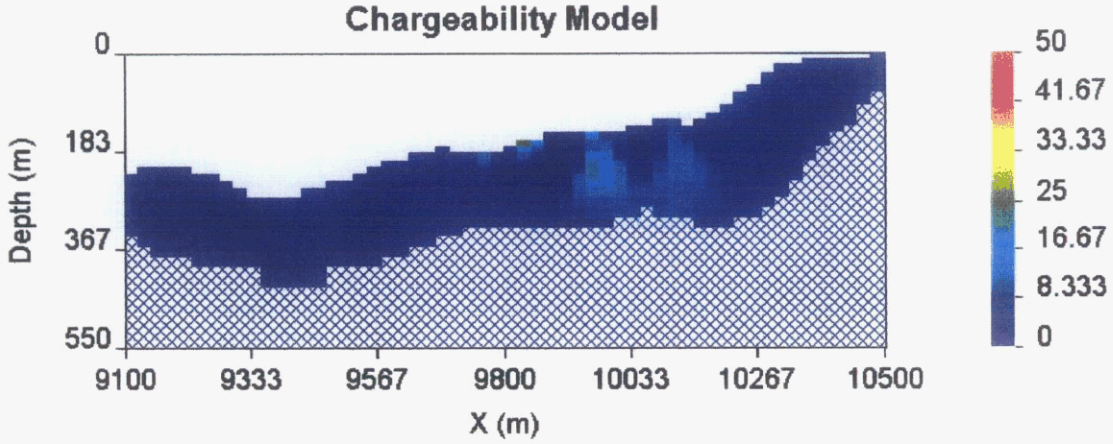

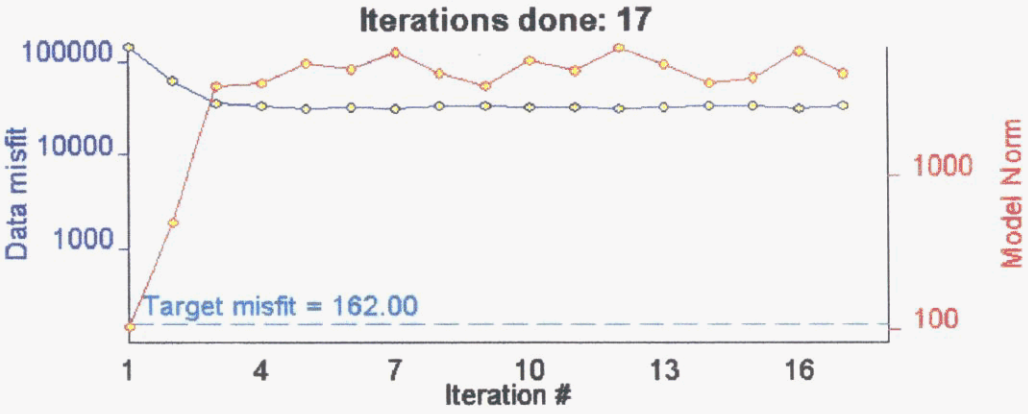

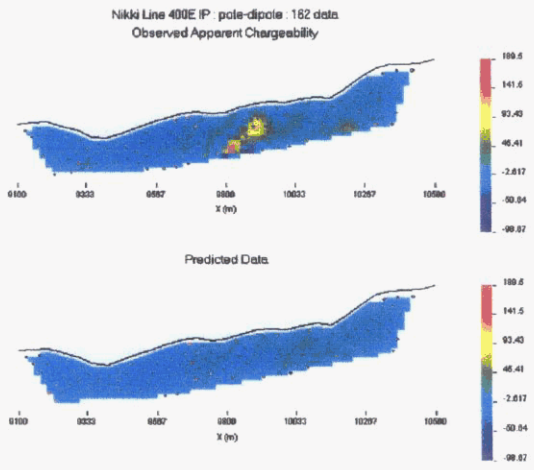

LINE 500E - RESISTIVITY

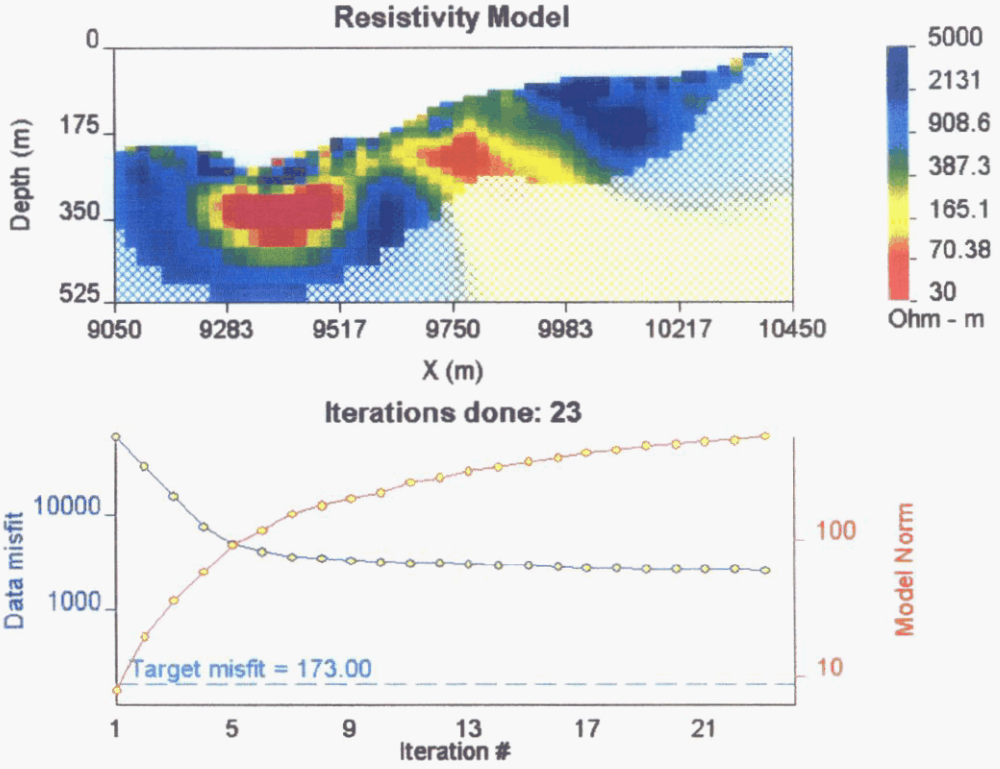

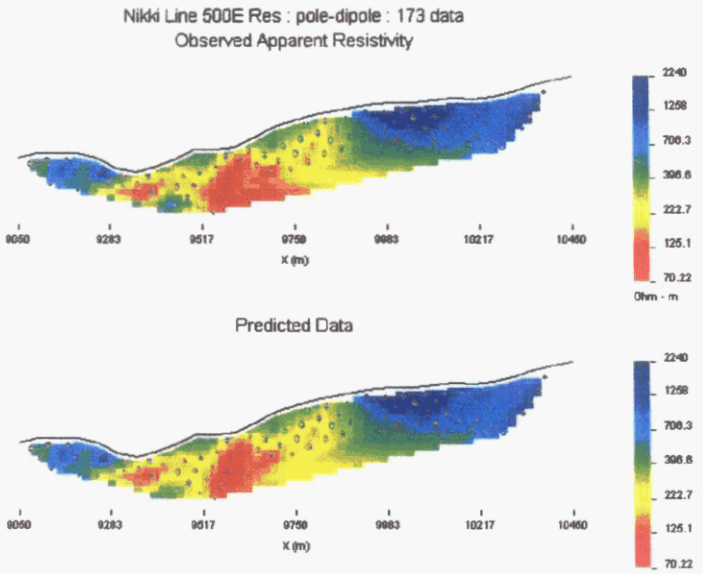

LINE 500E - CHARGEABILITY

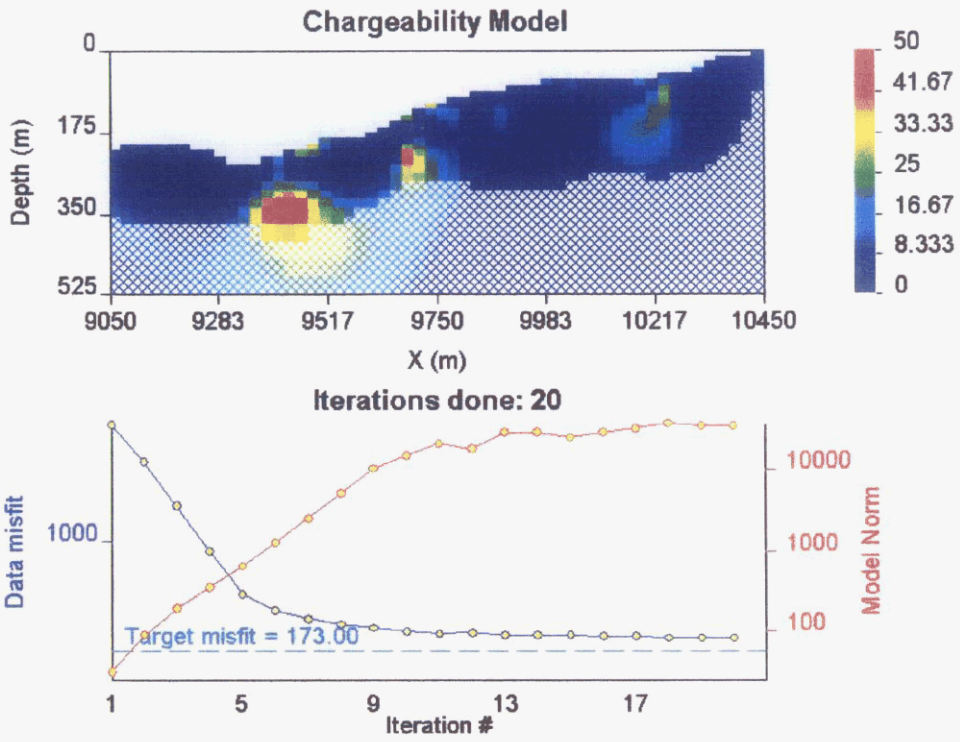

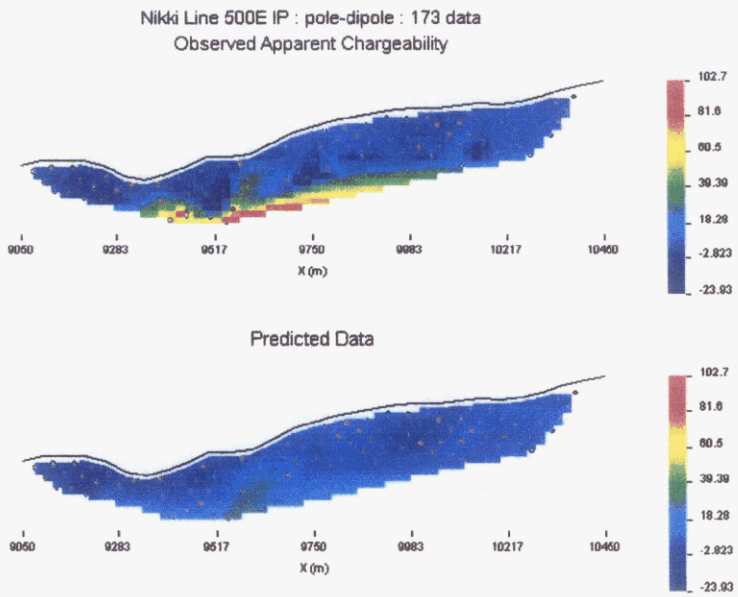

LINE 600E - RESISTIVITY

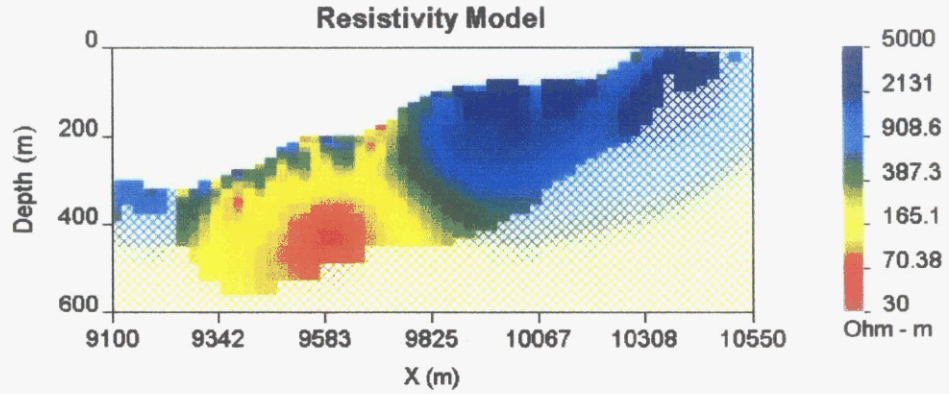

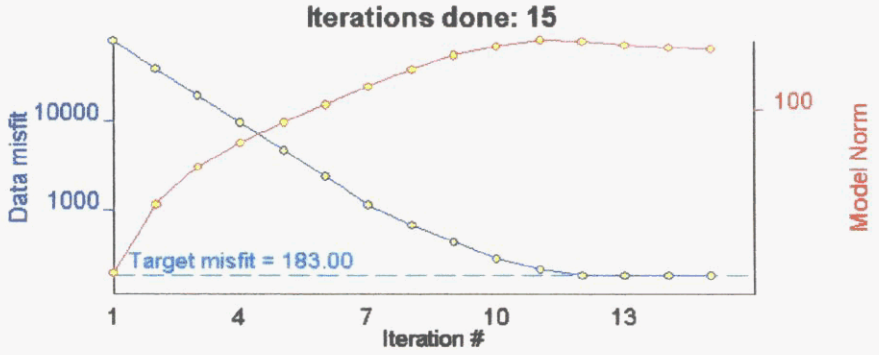

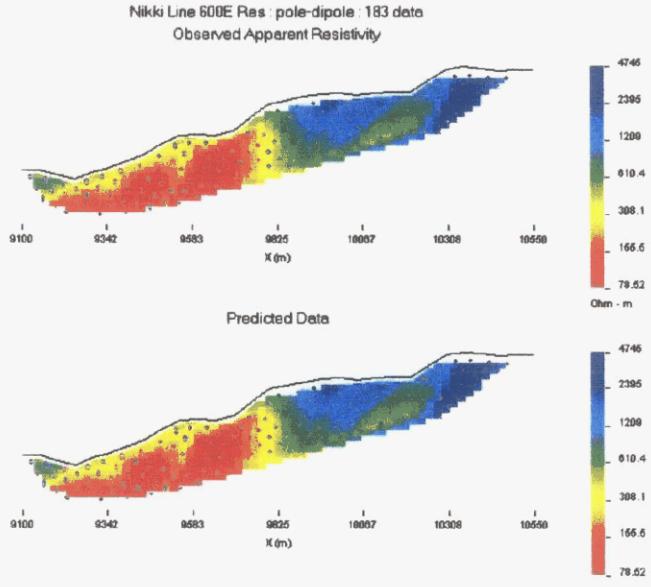

LINE 600E - CHARGEABILITY

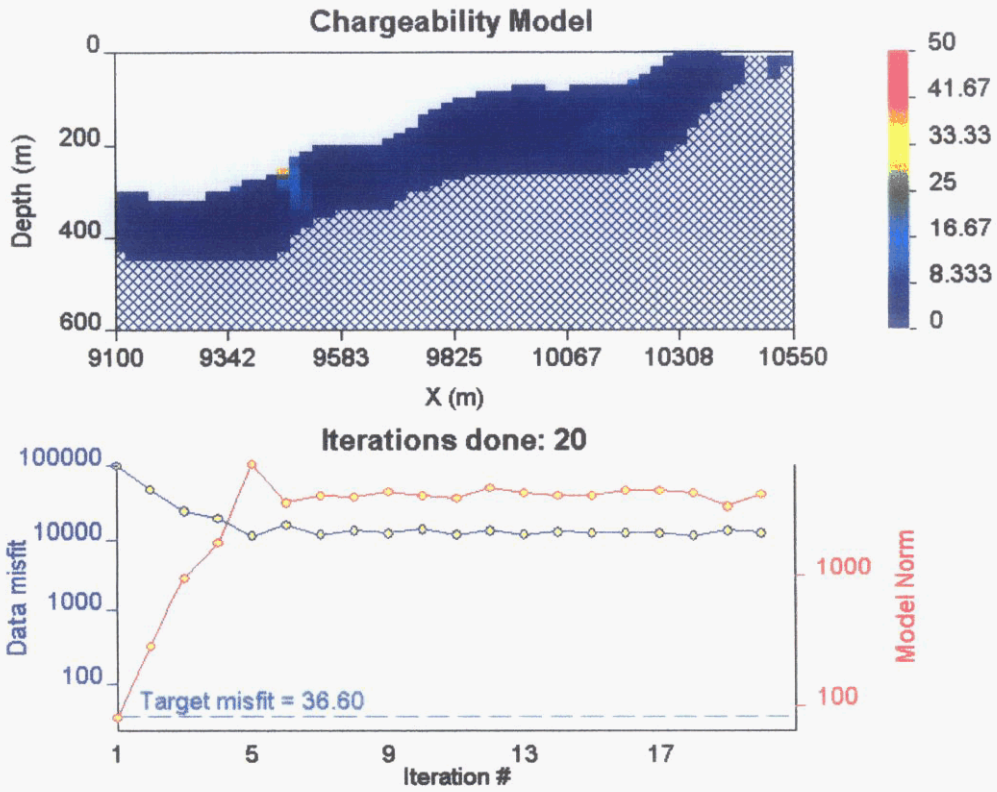

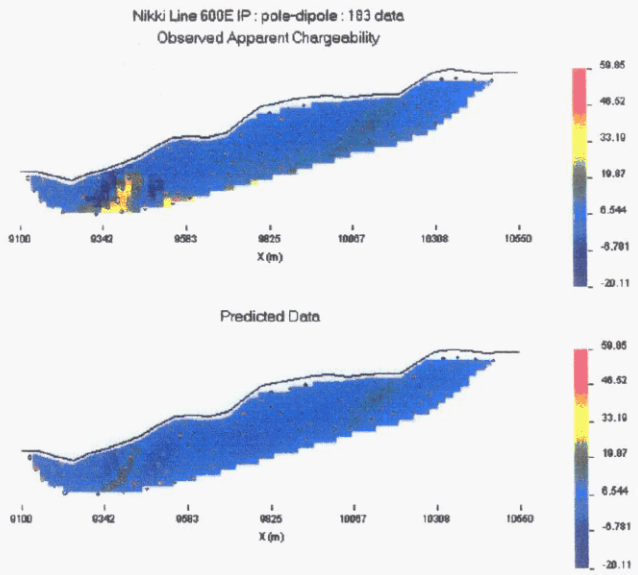

LINE 700E - RESISTIVITY

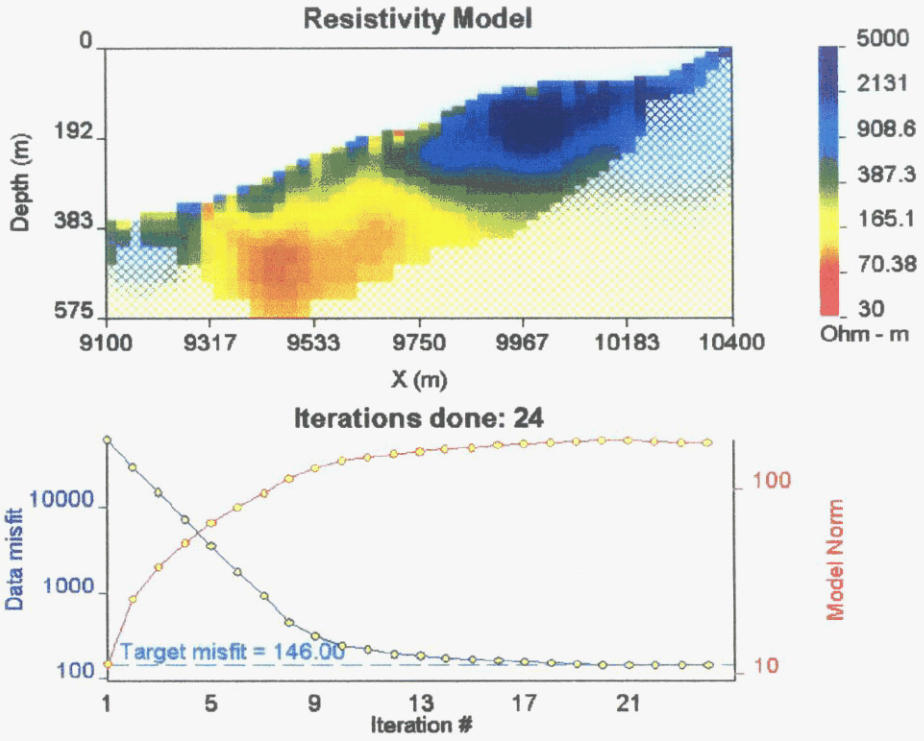

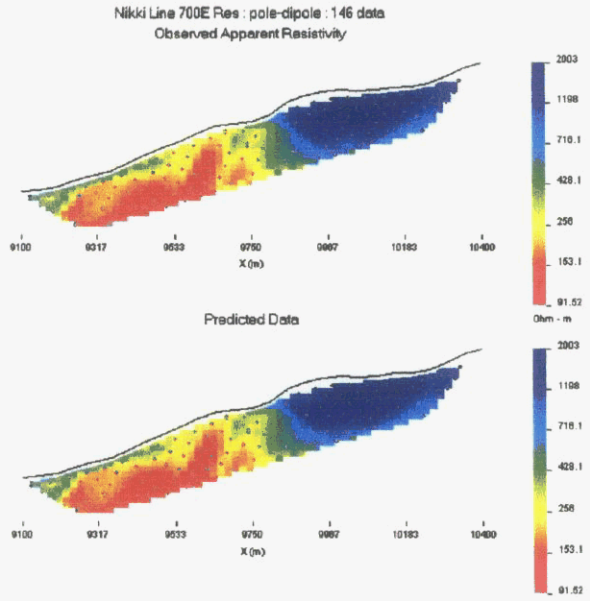

LINE 700E - CHARGEABILITY

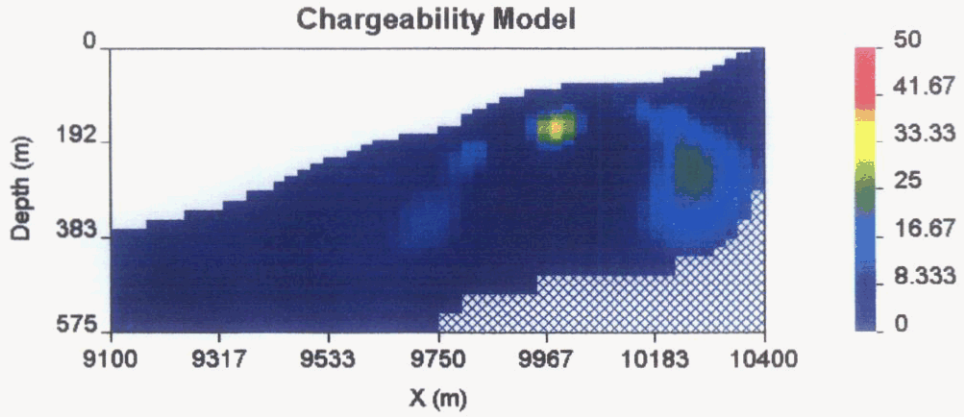

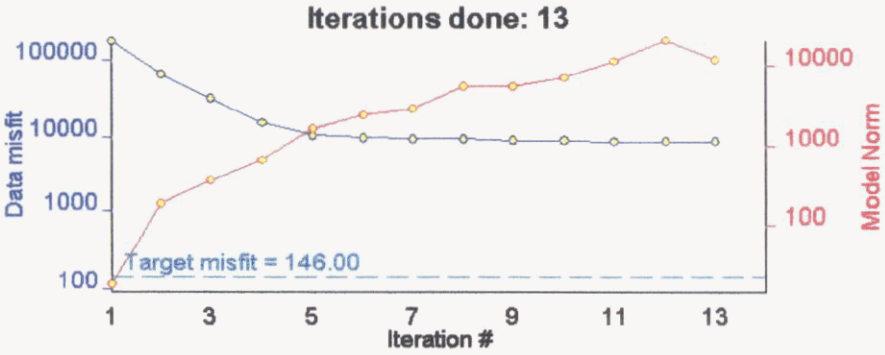

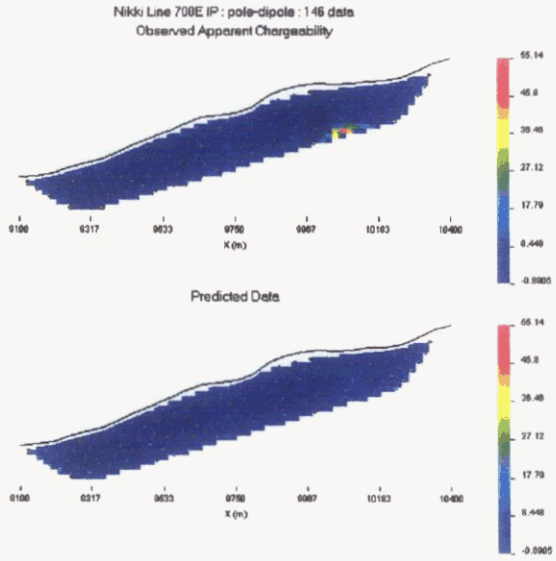

LINE 800E - RESISTIVITY

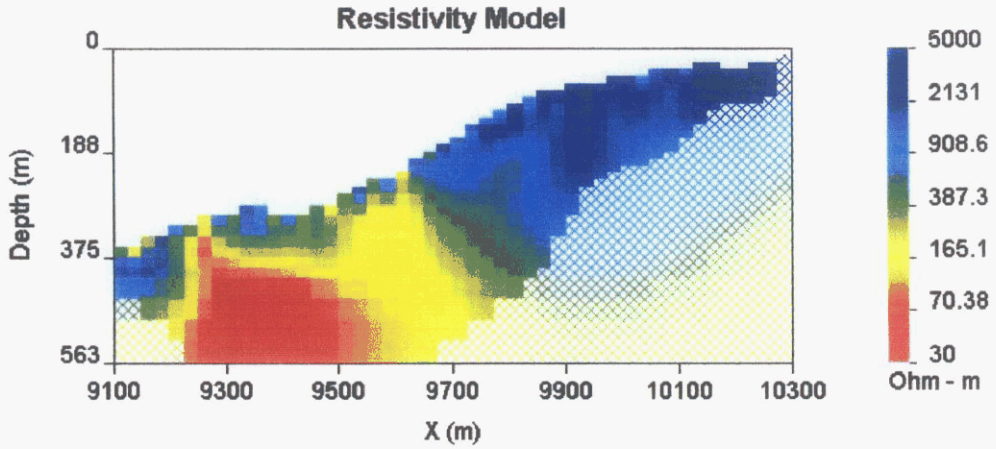

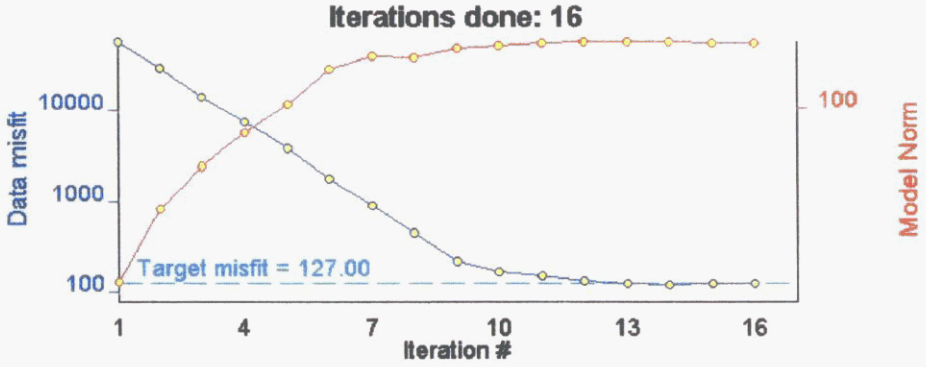

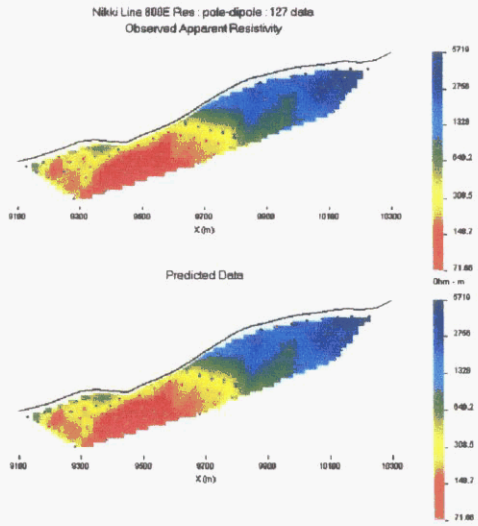

LINE 800E - CHARGEABILITY

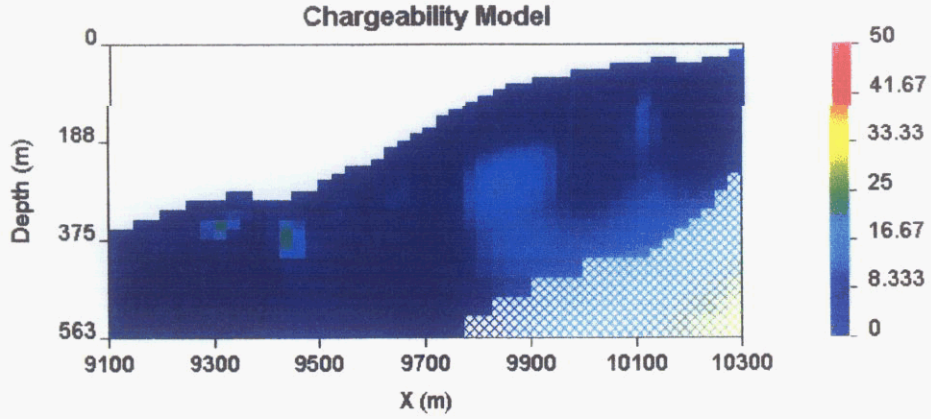

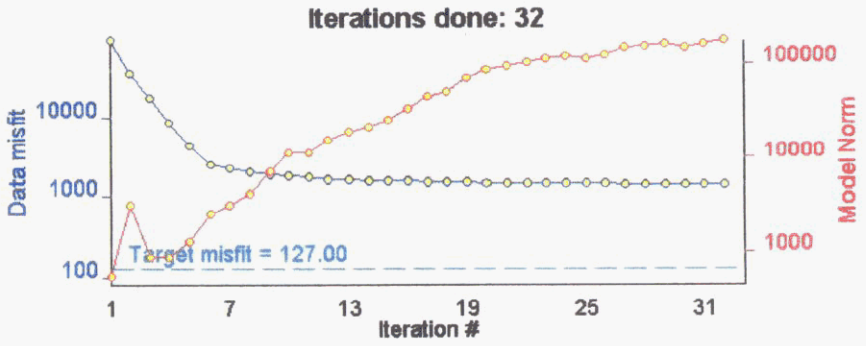

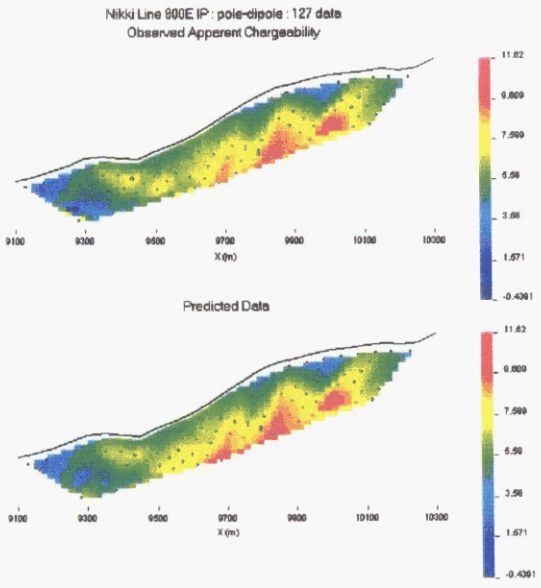

LINE 900E - RESISTIVITY

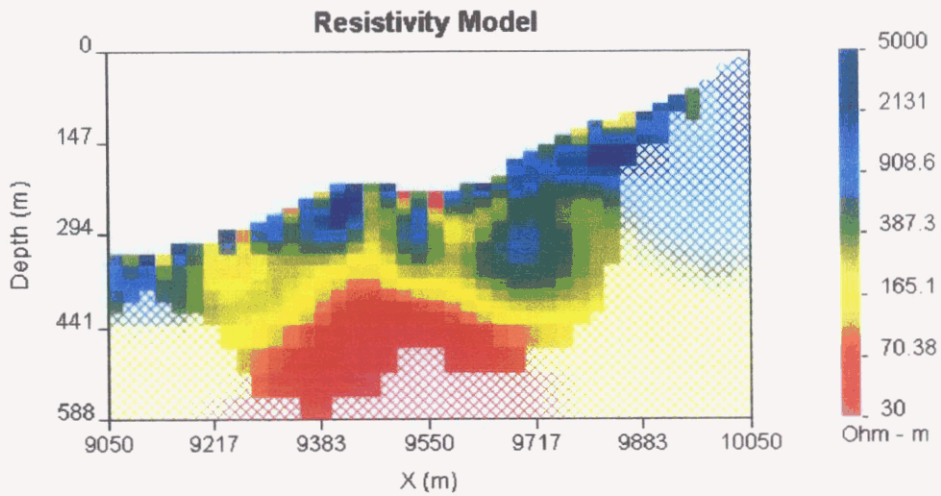

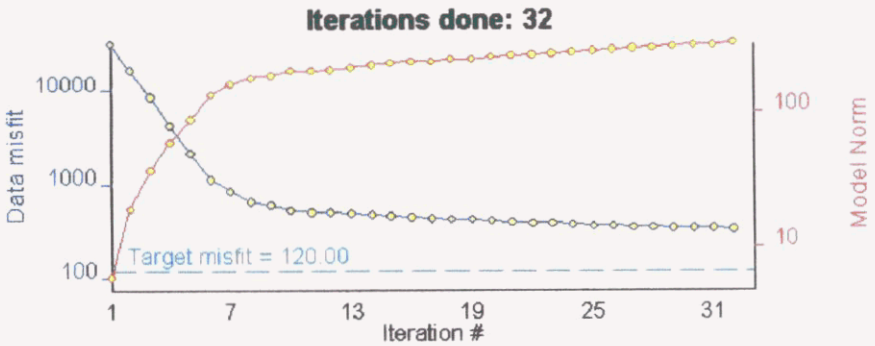

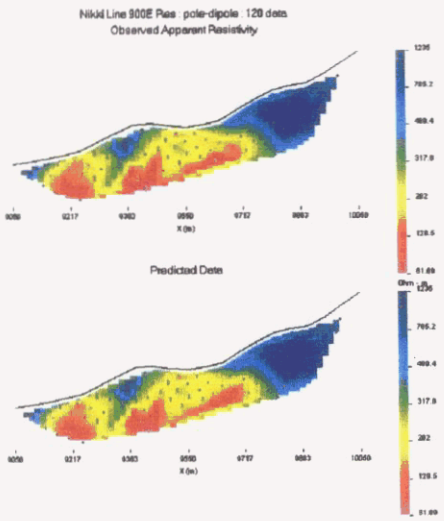

LINE 900E - CHARGEABILITY

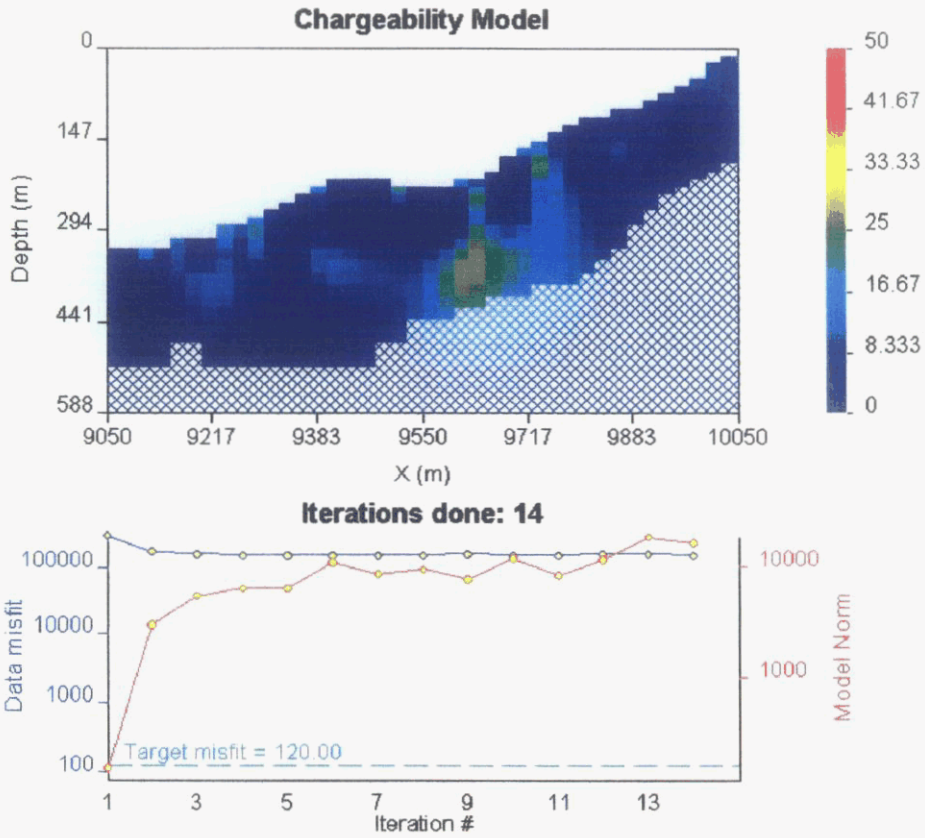

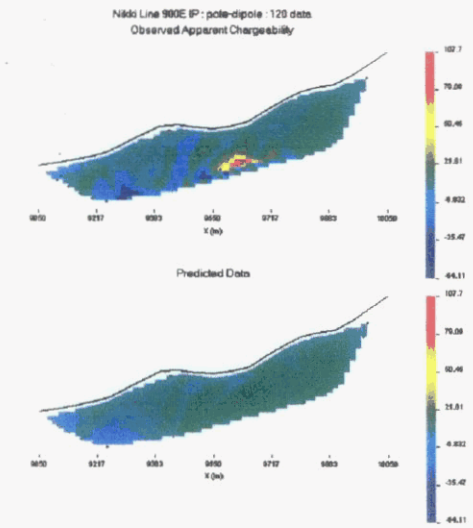

LINE 1000E - RESISTIVITY

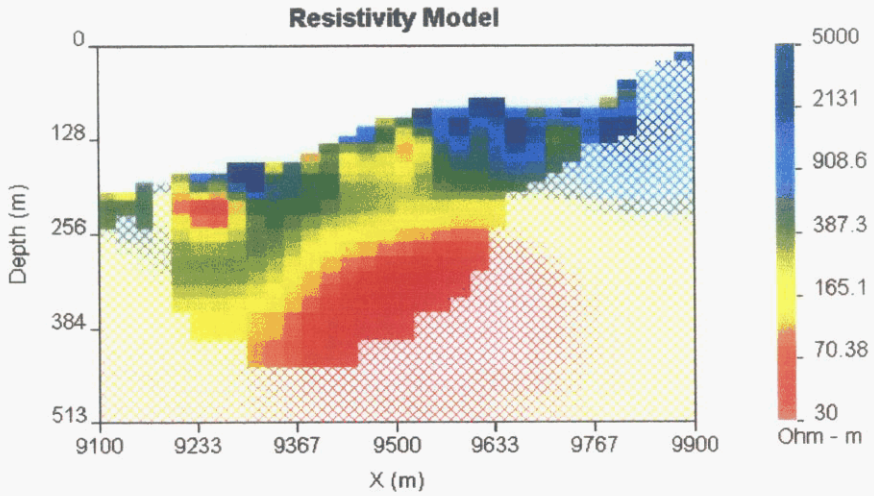

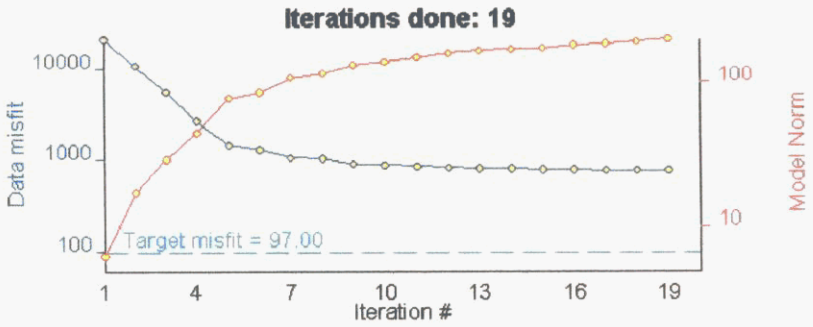

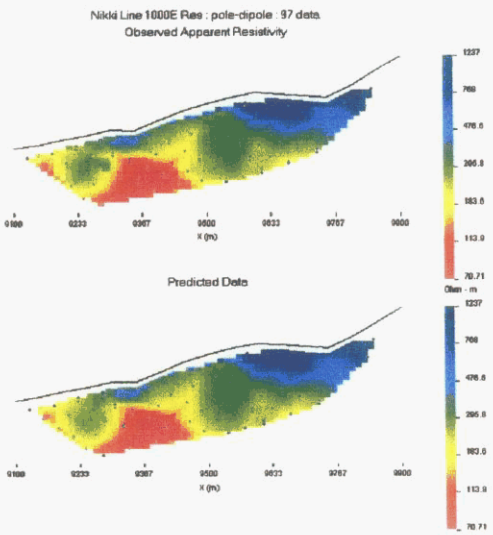

LINE 1000E - CHARGEABILITY

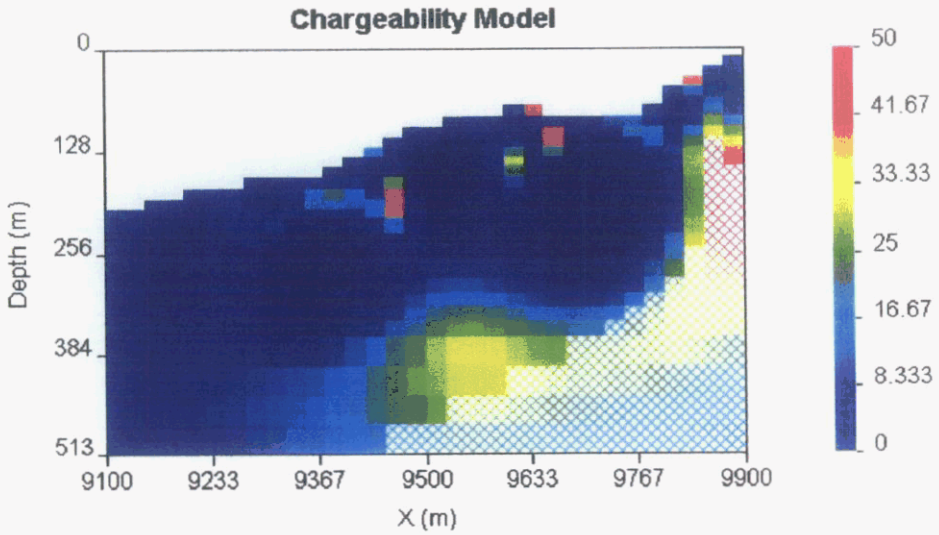

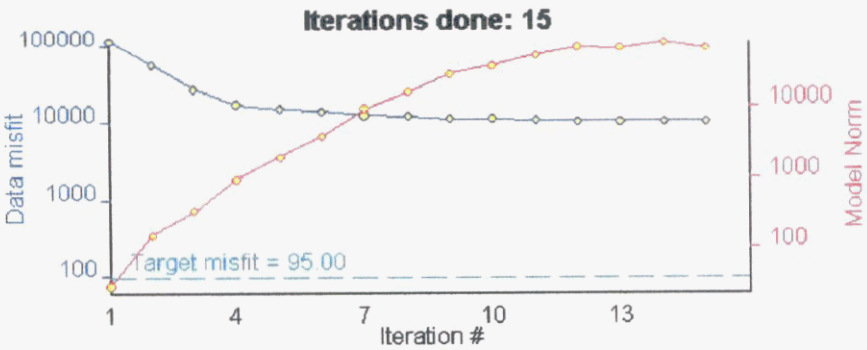

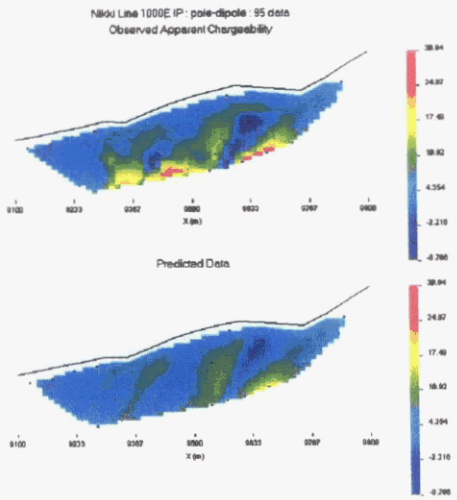

LINE 1100E - RESISTIVITY

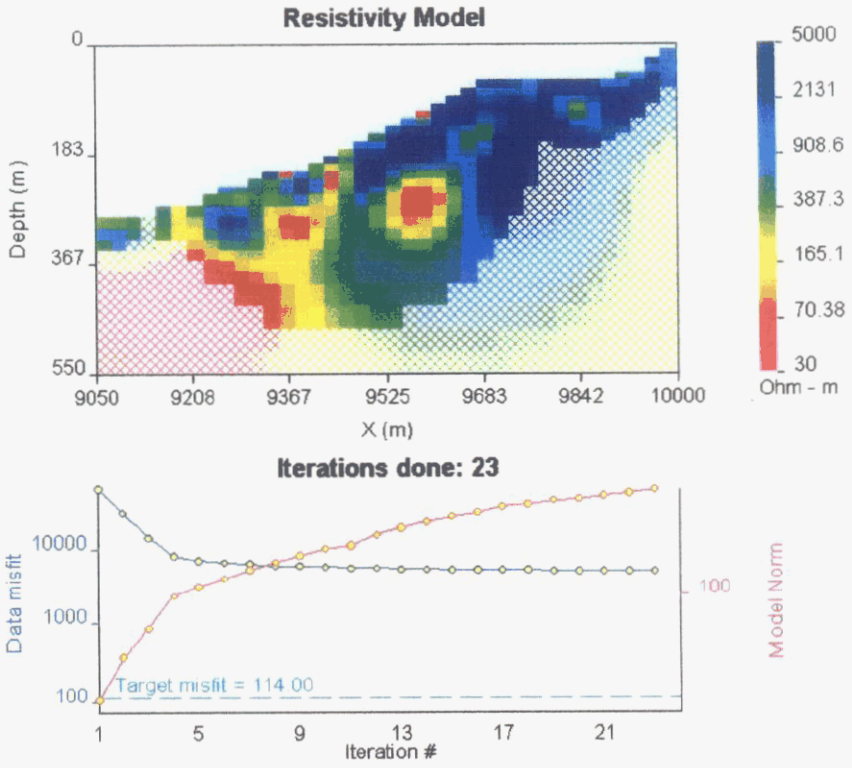

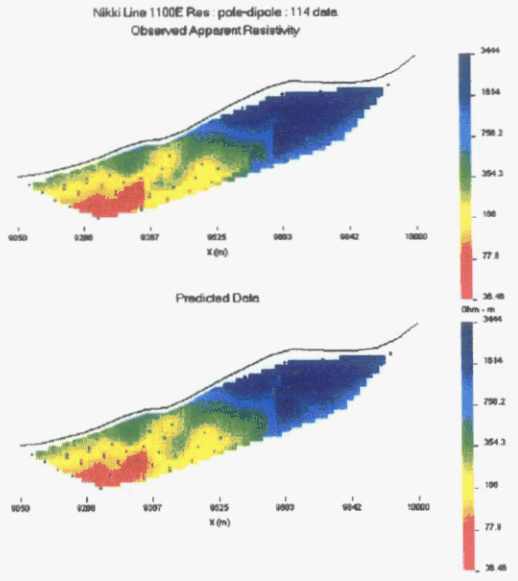

LINE 1100E - CHARGEABILITY

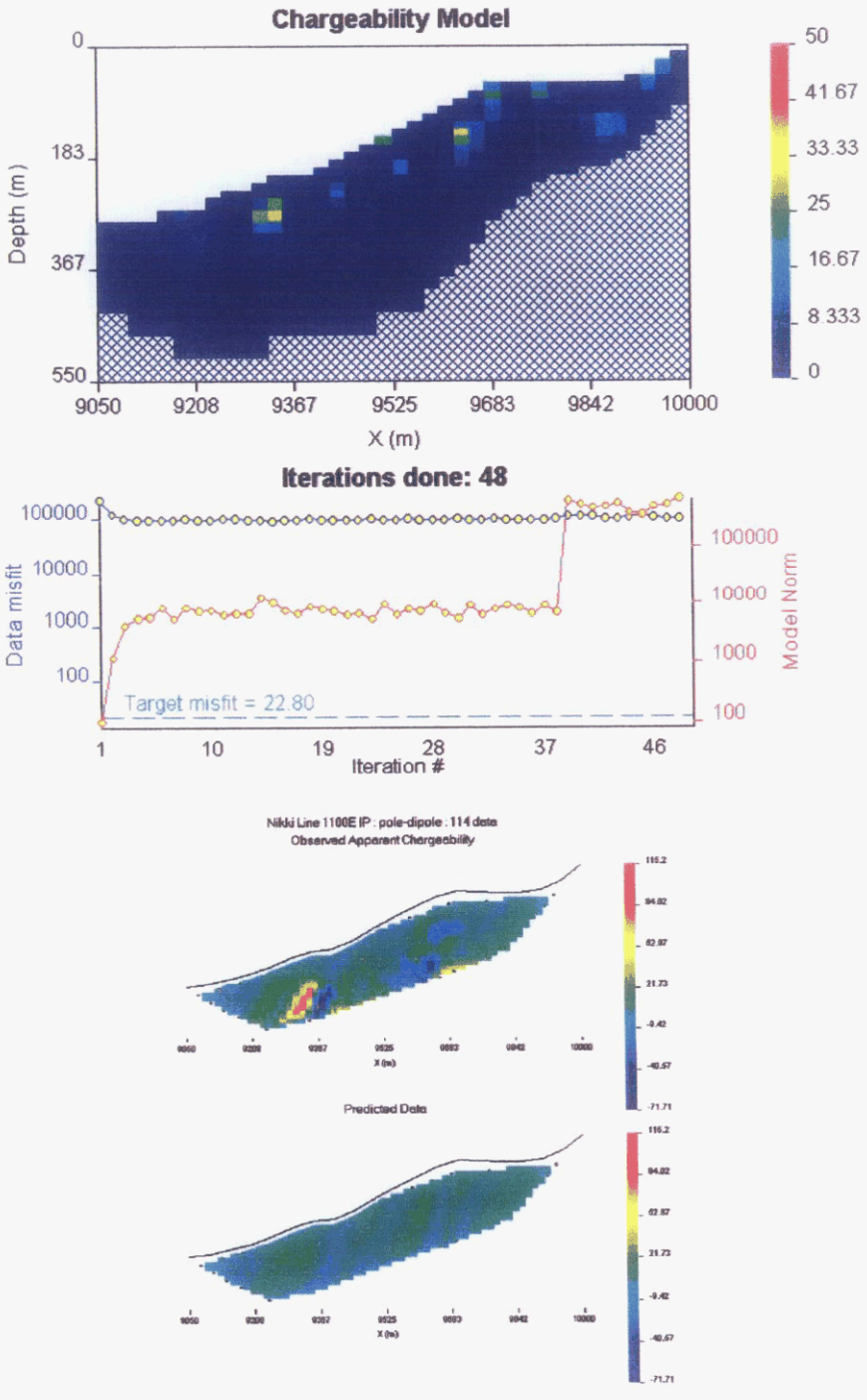

LINE 1200E - RESISTIVITY

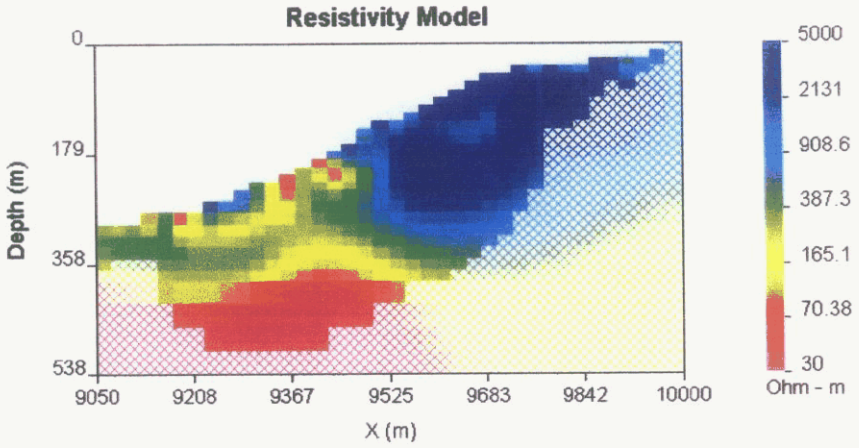

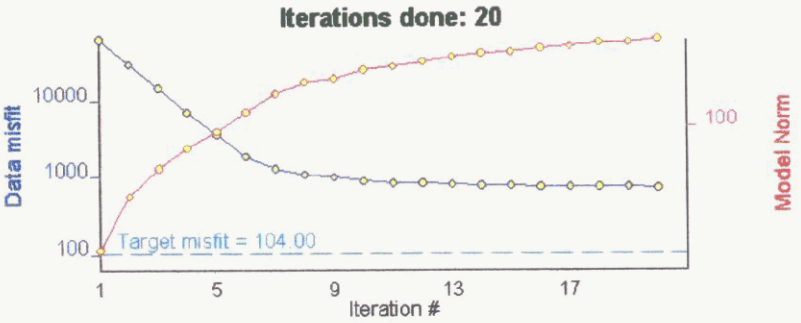

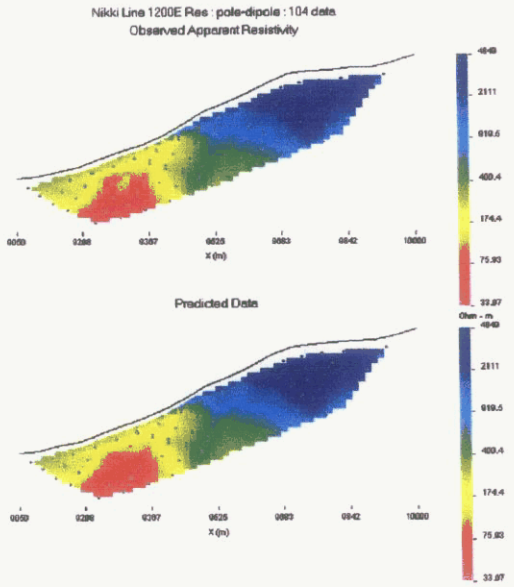

LINE 1200E - CHARGEABILITY

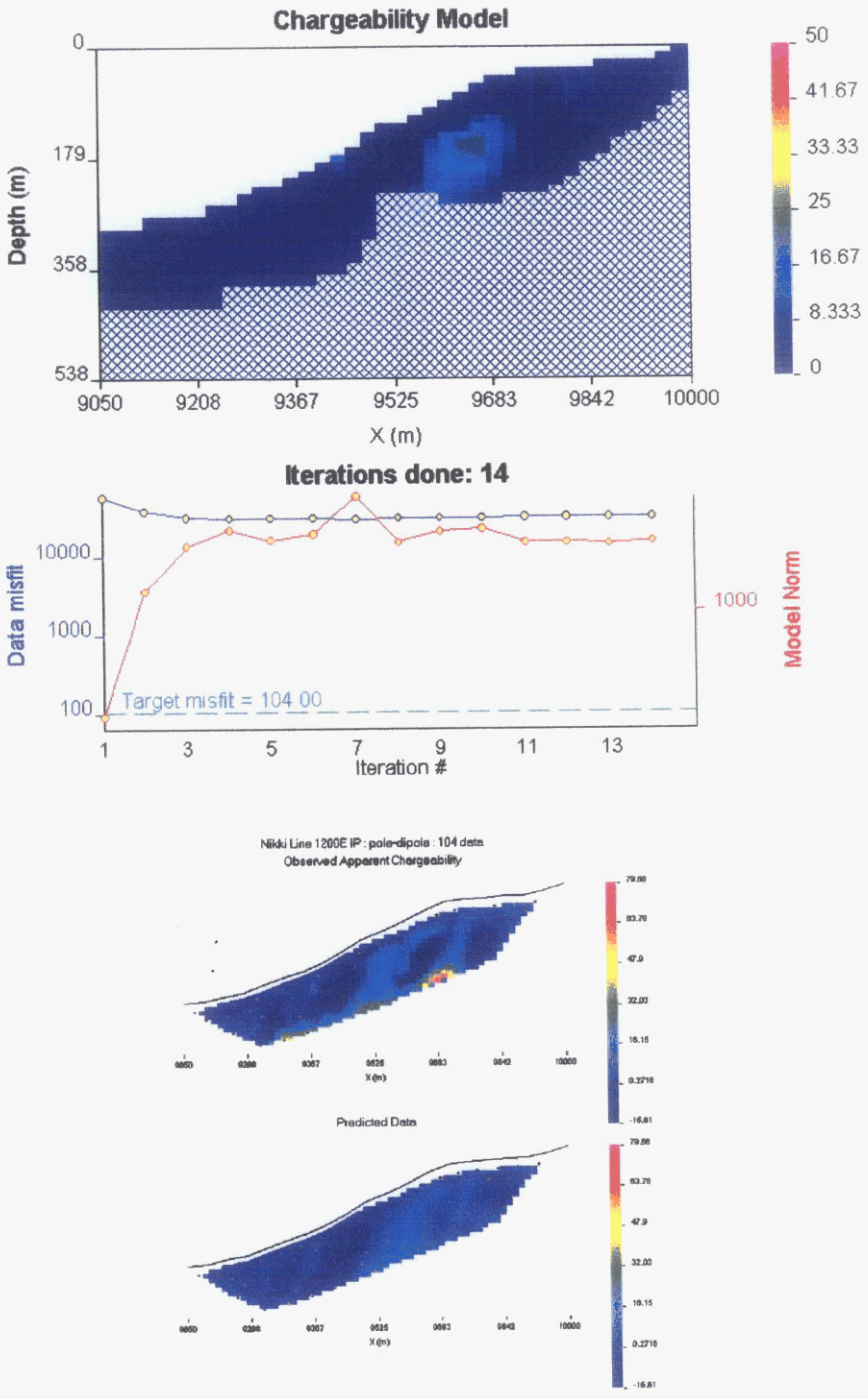

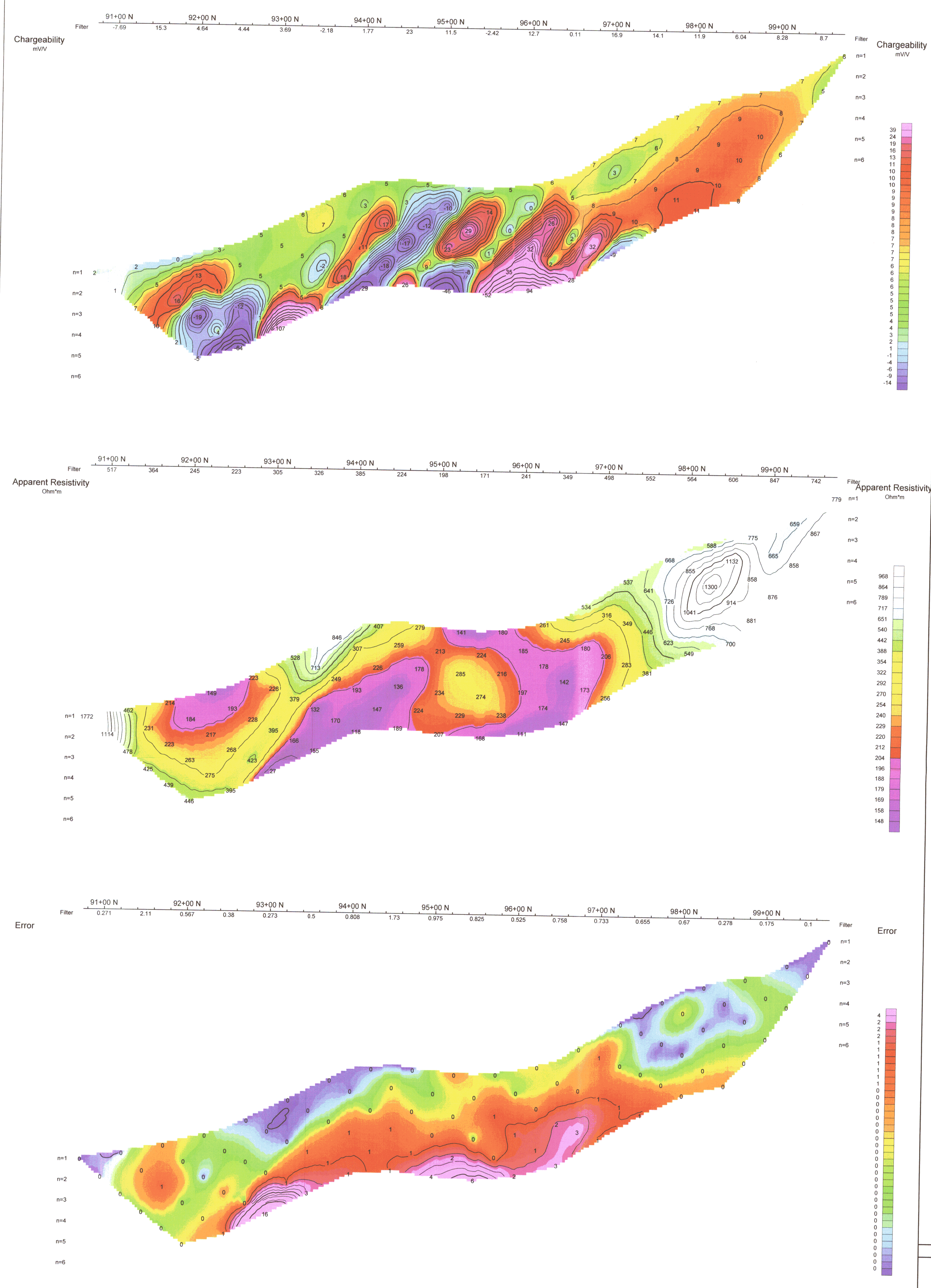

Pseudo Section Plot

9+00 E

Pole-Dipole Array

Pant-leg Filter

plot point

a = 50 m

INTERPRETATION

- ■ Strong increase in polarization accompanied by marked decrease in resistivity.
- ◘ Well defined increase in polarization without marked resistivity decrease.
- □ Poorly defined polarization increase with no resistivity signature.
- ▼ Low resistivity feature.

Scale 1:2500

25 0 25 50 75 100 125 150

metres

ATAC Resources Ltd.

INDUCED POLARIZATION SURVEY

Nicki Grid

Line 900E

Date: 07/10/2004

Interpretation:

Aurora Geosciences Ltd.

Pseudo Section Plot
10+00 E

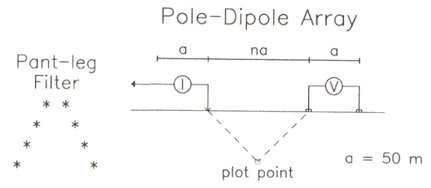

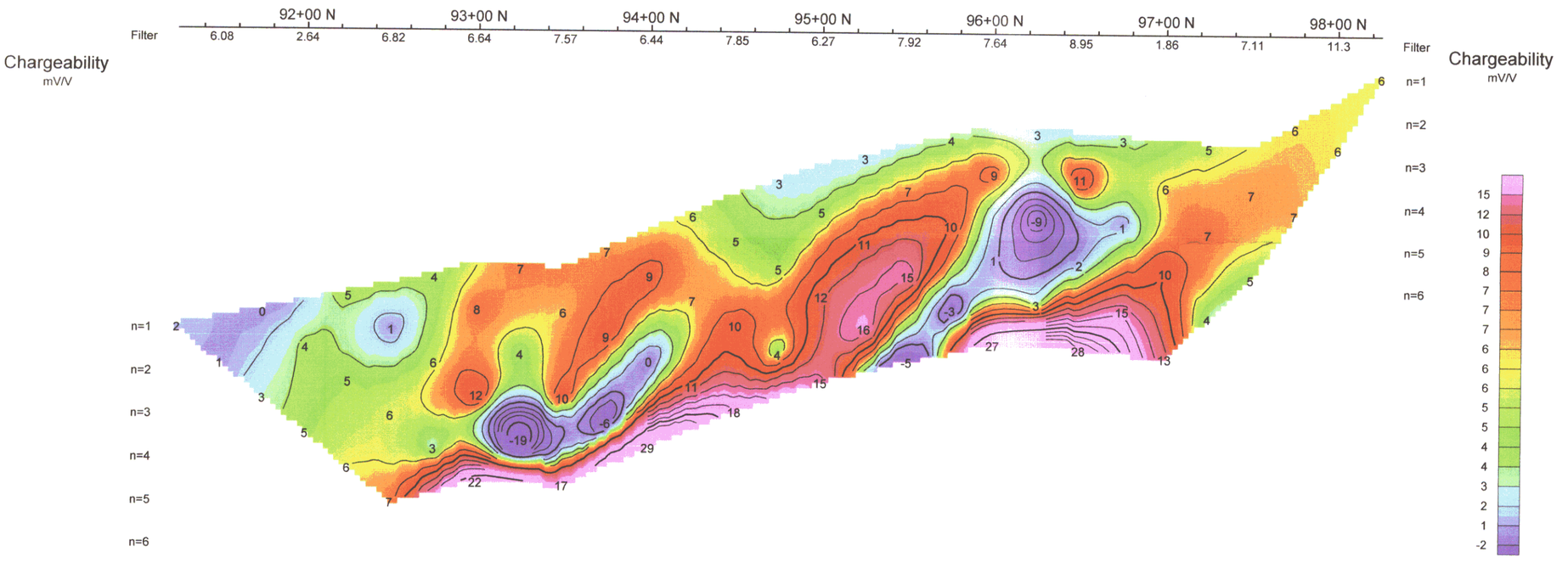

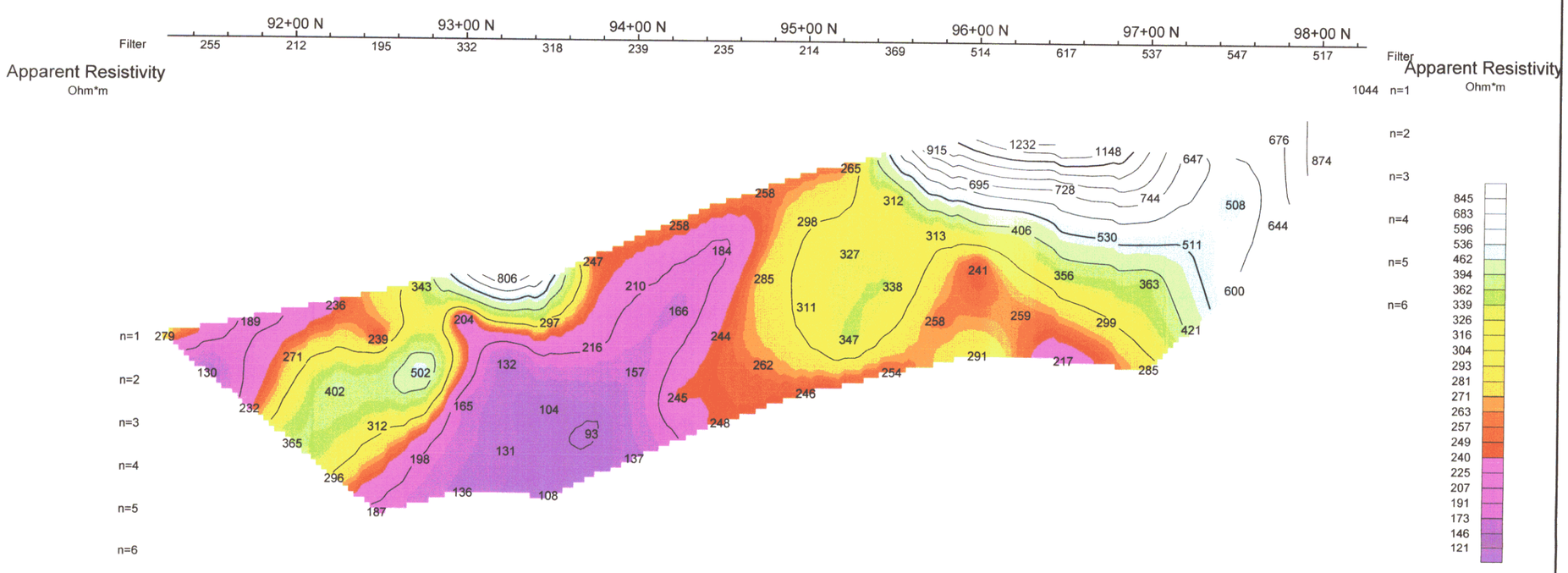

INTERPRETATION

- ■ Strong increase in polarization accompanied by marked decrease in resistivity.
- ▣ Well defined increase in polarization without marked resistivity decrease.
- □ Poorly defined polarization increase with no resistivity signature.
- ▼ Low resistivity feature.

094527

Scale 1:2500

25 0 25 50 75 100 125 150
metres

ATAC Resources Ltd.

INDUCED POLARIZATION SURVEY
Nicki Grid
Line 1000E

Date: 07/10/2004
Interpretation:

Aurora Geosciences Ltd.

Pseudo Section Plot
11+00 E

Pole-Dipole Array

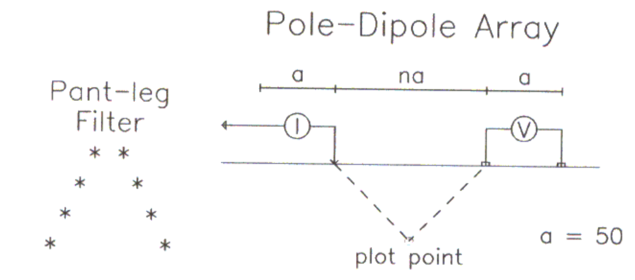

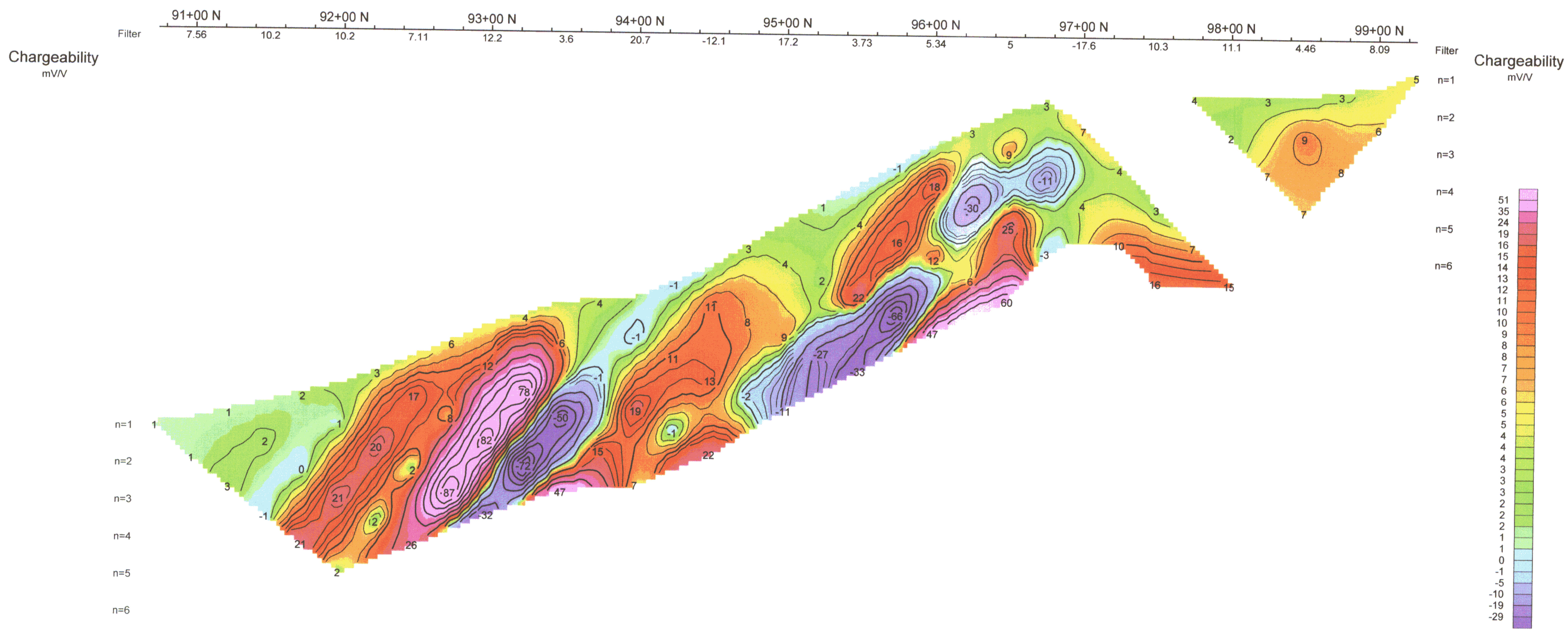

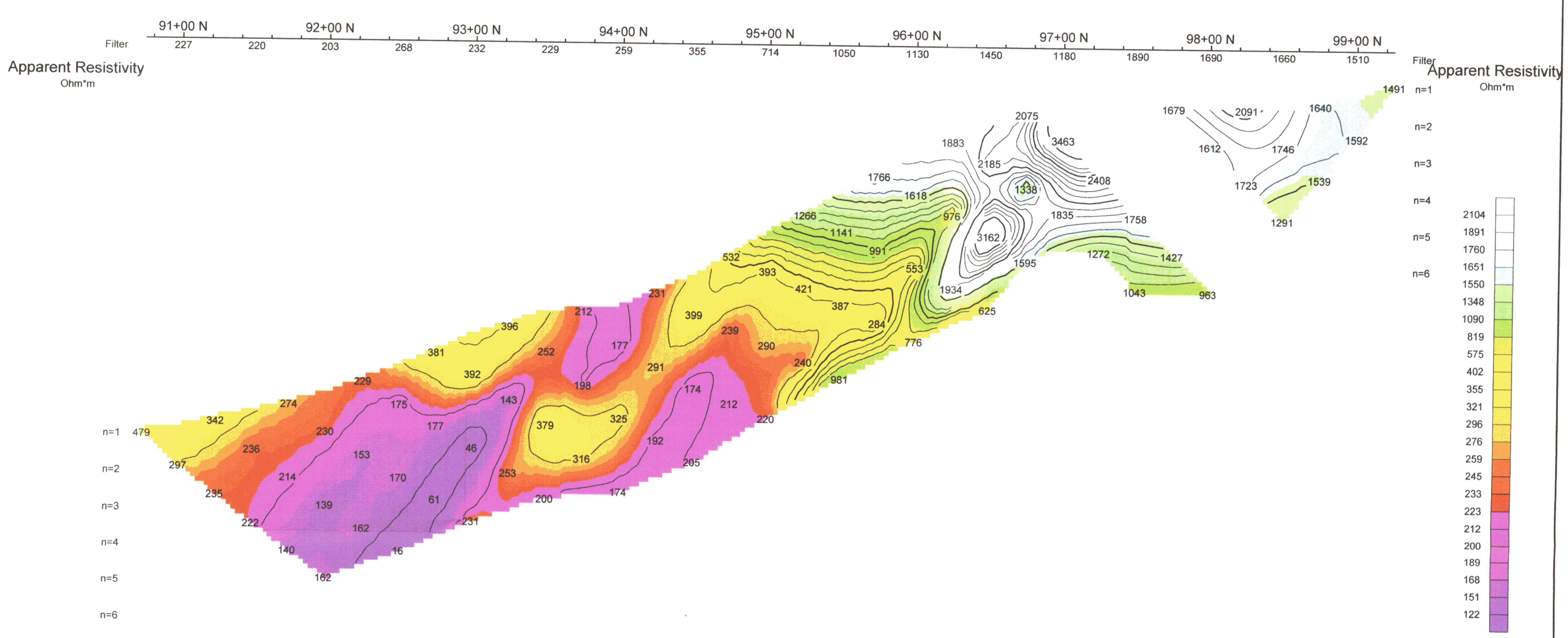

INTERPRETATION

- ■ Strong increase in polarization accompanied by marked decrease in resistivity.
- □ Well defined increase in polarization without marked resistivity decrease.
- □ Poorly defined polarization increase with no resistivity signature.
- ▼ Low resistivity feature.

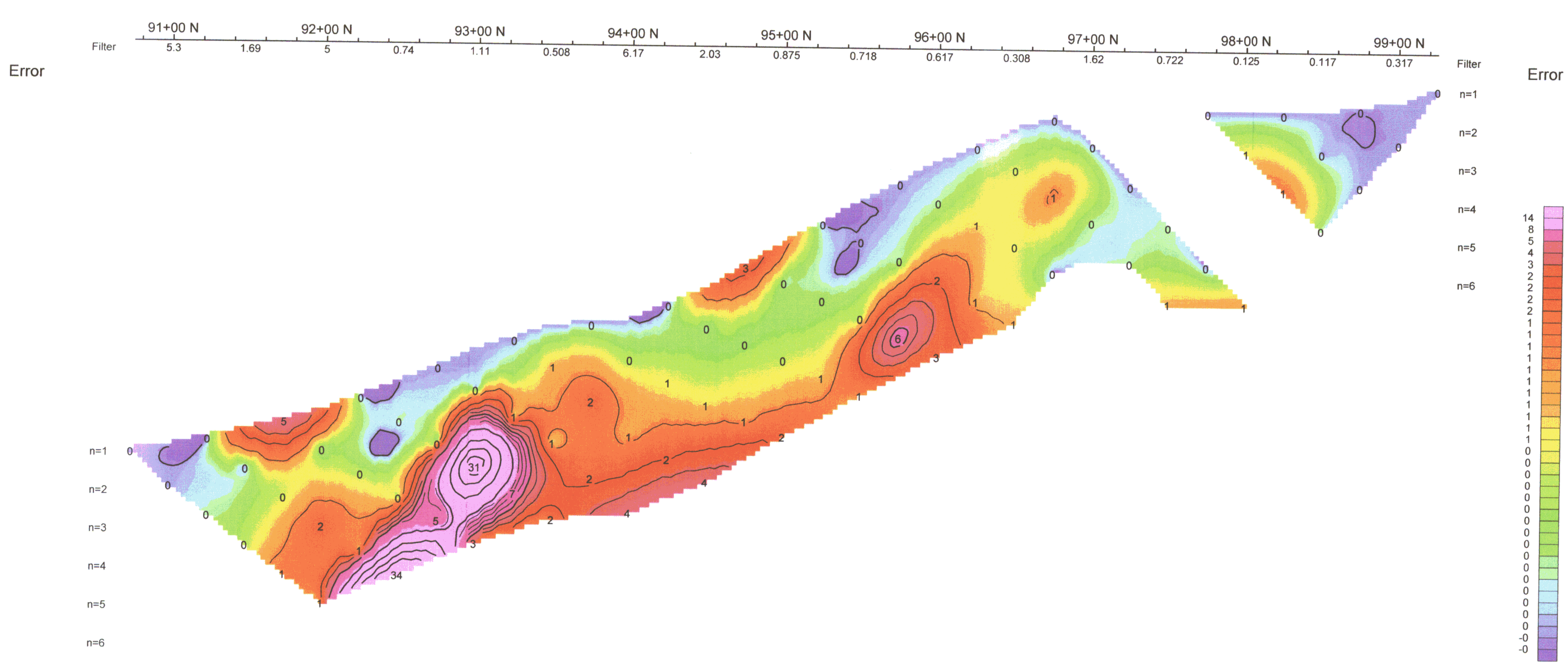

Scale 1:2500

25 0 25 50 75 100 125 150
metres

ATAC Resources Ltd.

INDUCED POLARIZATION SURVEY

Nicki Grid

Line 1100E

Date: 07/10/2004

Interpretation:

Aurora Geosciences Ltd.

Pseudo Section Plot
12+00 E

Pole-Dipole Array

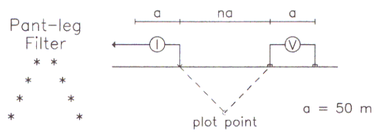

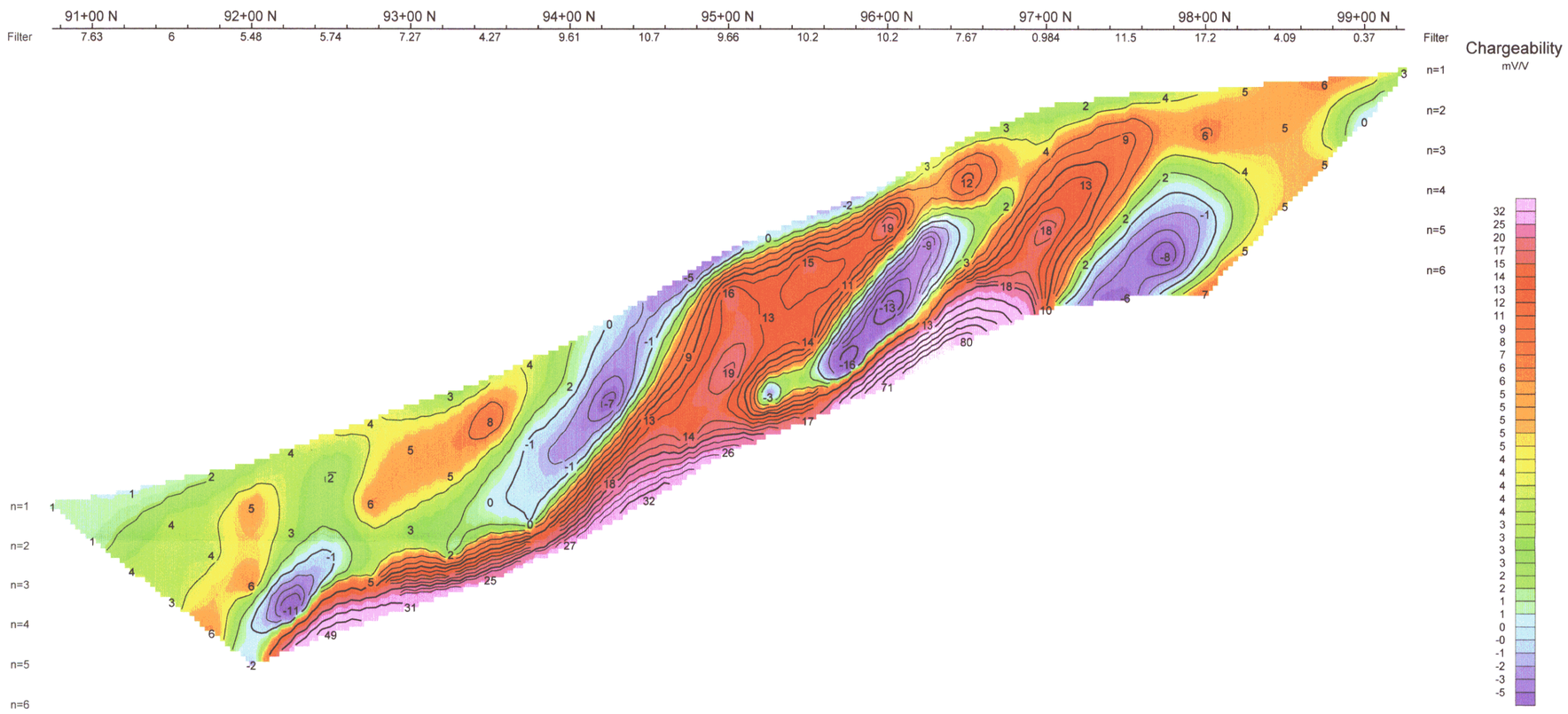

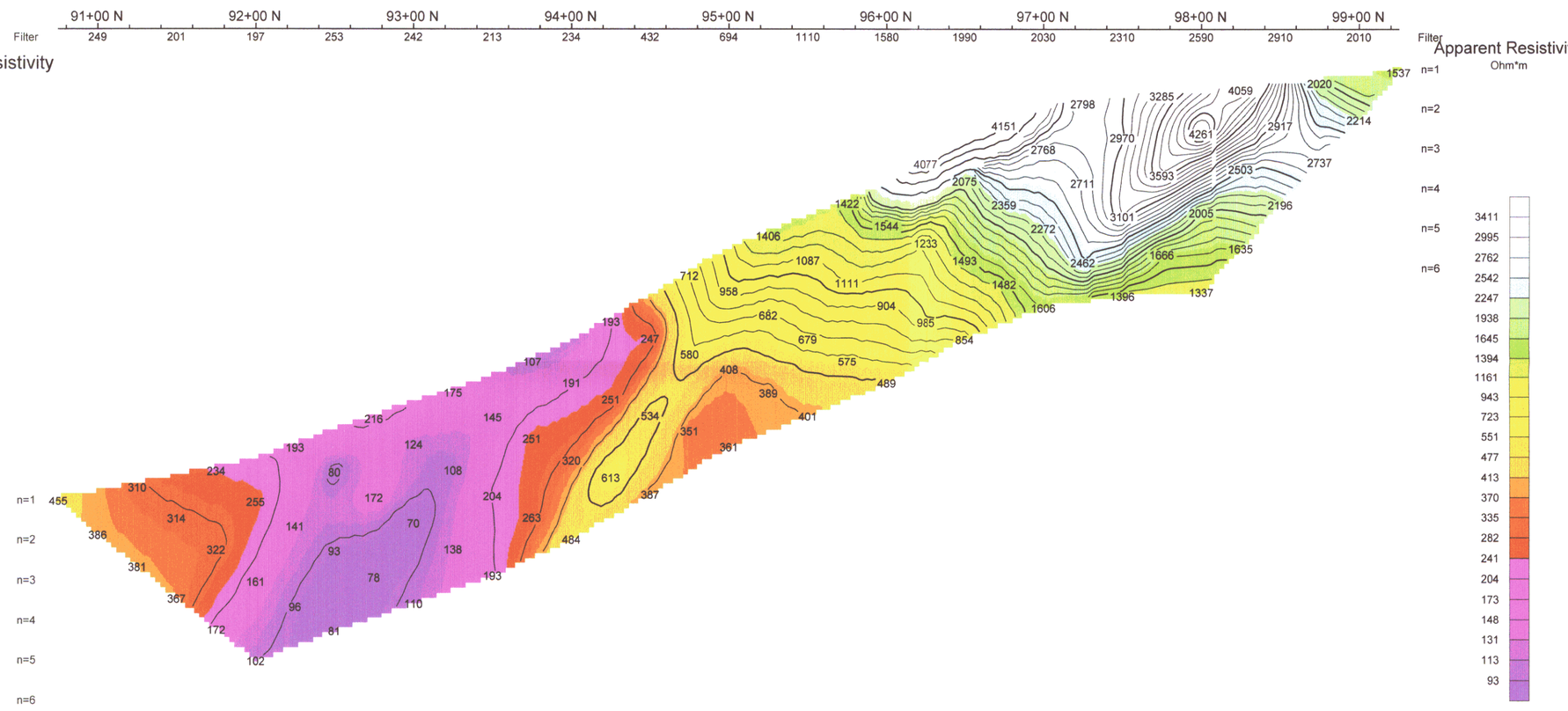

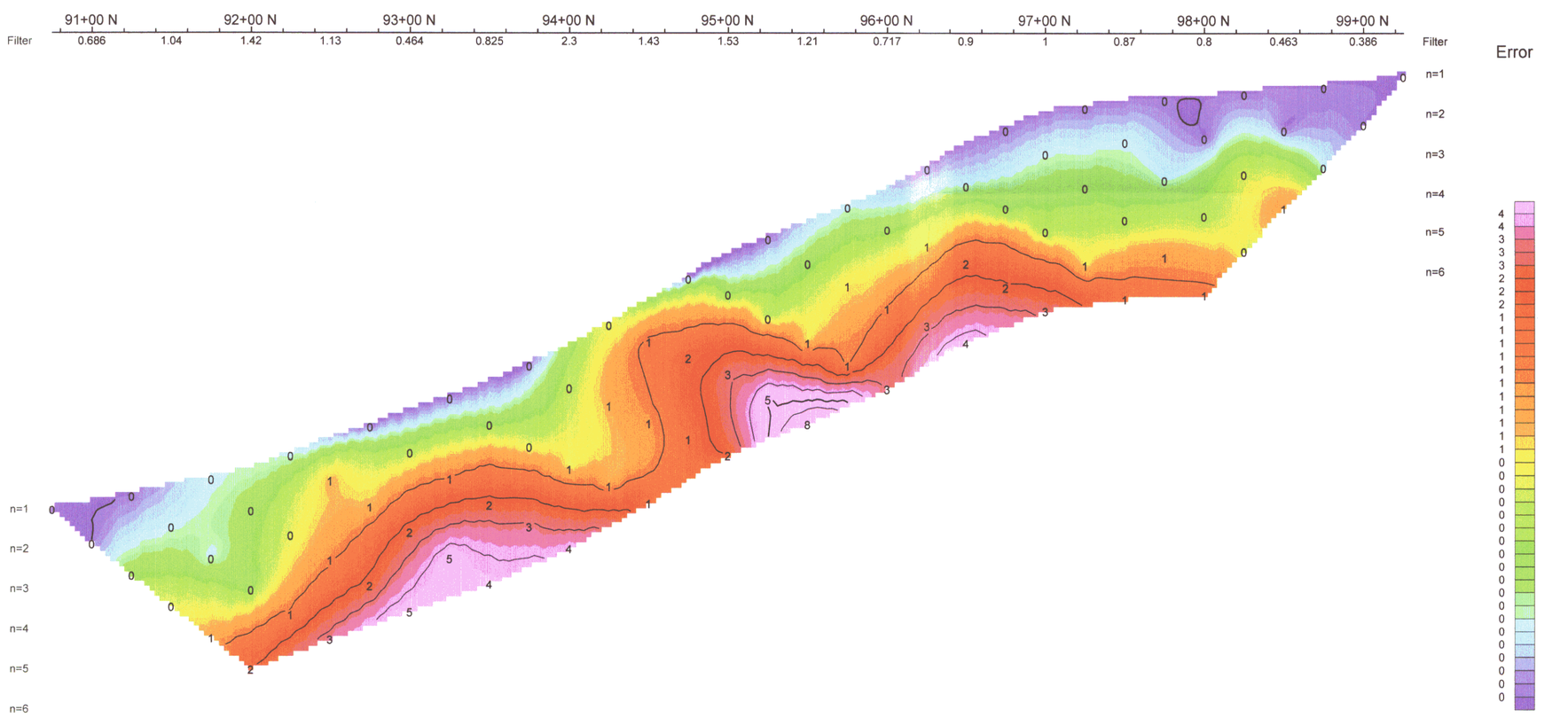

INTERPRETATION

- ■ Strong increase in polarization accompanied by marked decrease in resistivity.
- □ Well defined increase in polarization without marked resistivity decrease.
- □ Poorly defined polarization increase with no resistivity signature.
- ▼ Low resistivity feature.

Scale 1:2500

25 0 25 50 75 100 125 150
metres

ATAC Resources Ltd.

INDUCED POLARIZATION SURVEY
Nicki Grid
Line 1200E

Date: 07/10/2004
Interpretation:

Aurora Geosciences Ltd.

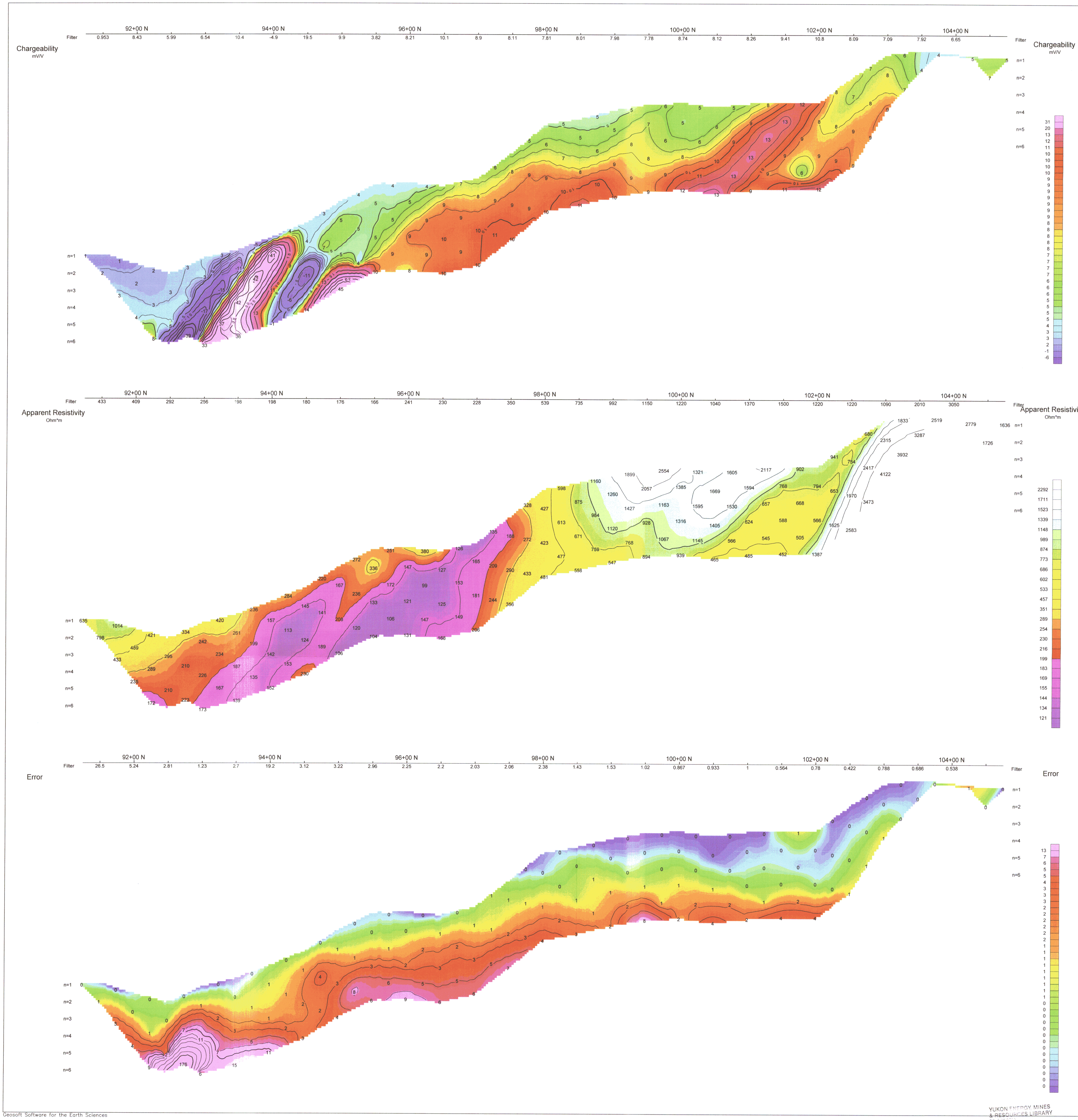

Pseudo Section Plot
6+00 E

Pole-Dipole Array

Pant-leg Filter

plot point

a = 50 m

Logarithmic Contours 1, 1.5, 2, 3, 5, 7.5, 10, ...

INTERPRETATION

- ■ Strong increase in polarization accompanied by marked decrease in resistivity.
- ◘ Well defined increase in polarization without marked resistivity decrease.
- □ Poorly defined polarization increase with no resistivity signature.
- ▼ Low resistivity feature.

094527

Scale 1:2500

25 0 25 50 75 100 125 150

metres

ATAC Resources Ltd.

INDUCED POLARIZATION SURVEY

Nicki Grid

Line 600E

Date: 07/10/2004

Interpretation:

Aurora Geosciences Ltd.

Pseudo Section Plot
7+00 E

Pole-Dipole Array

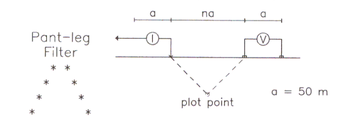

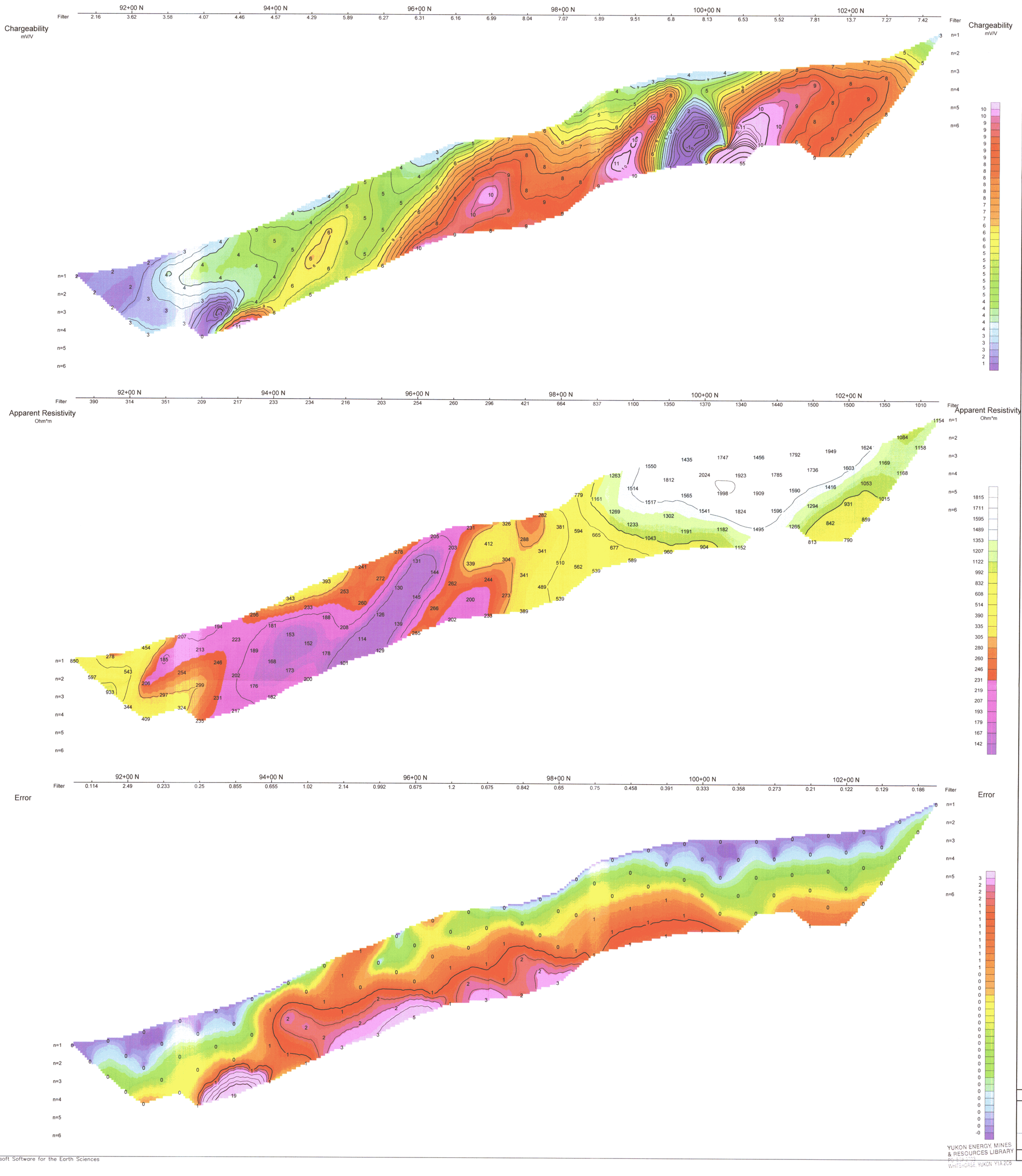

Logarithmic Contours 1, 1.5, 2, 3, 5, 7.5, 10, . . .

INTERPRETATION

- ■ Strong increase in polarization accompanied by marked decrease in resistivity.
- □ Well defined increase in polarization without marked resistivity decrease.
- □ Poorly defined polarization increase with no resistivity signature.
- ▼ Low resistivity feature.

094527

REGISTERED PROFESSIONAL GEOPHYSICIST
M. A. POWER
LICENSEE
30 NOV 04
N.W.T.

Scale 1:2500

25 0 25 50 75 100 125 150
metres

ATAC Resources Ltd.

INDUCED POLARIZATION SURVEY
Nicki Grid
Line 700E

Date: 07/10/2004
Interpretation:

Aurora Geosciences Ltd.

Pseudo Section Plot
8+00 E

Pole-Dipole Array

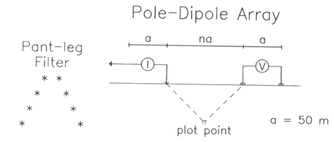

INTERPRETATION

- ■ Strong increase in polarization accompanied by marked decrease in resistivity.
- □ Well defined increase in polarization without marked resistivity decrease.
- □ Poorly defined polarization increase with no resistivity signature.
- ▼ Low resistivity feature.

094527

REGISTERED PROFESSIONAL GEOPHYSICIST
M.A. POWER
LICENSEE
30 NOV 04
N.W.T.

Scale 1:2500

25 0 25 50 75 100 125 150
metres

ATAC Resources Ltd.

INDUCED POLARIZATION SURVEY
Nicki Grid
Line 800E

Date: 07/10/2004
Interpretation:

Aurora Geosciences Ltd.

Pseudo Section Plot
5+00 E

Pole-Dipole Array

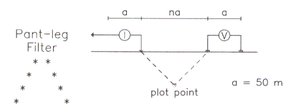

Logarithmic Contours 1, 1.5, 2, 3, 5, 7.5, 10,...

INTERPRETATION

- ■ Strong increase in polarization accompanied by marked decrease in resistivity.
- □ Well defined increase in polarization without marked resistivity decrease.
- □ Poorly defined polarization increase with no resistivity signature.
- ▼ Low resistivity feature.

094527

REGISTERED PROFESSIONAL GEOPHYSICIST
M.A. LOWER
LICENSEE
30 NOV 04
N.W.T.

Scale 1:2500

25 0 25 50 75 100 125 150
metres

ATAC Resources Ltd.

INDUCED POLARIZATION SURVEY
Nicki Grid
Line 500E

Date: 07/10/2004
Interpretation:

Aurora Geosciences Ltd.

Geosoft Software for the Earth Sciences

Pseudo Section Plot

4+00 E

Pole-Dipole Array

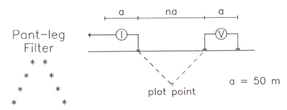

Logarithmic Contours 1, 1.5, 2, 3, 5, 7.5, 10, . . .

INTERPRETATION

- ■ Strong increase in polarization accompanied by marked decrease in resistivity.
- ▣ Well defined increase in polarization without marked resistivity decrease.
- □ Poorly defined polarization increase with no resistivity signature.
- ▼ Low resistivity feature.

094527

REGISTERED PROFESSIONAL GEOPHYSICIST
M. A. POWER
LICENSEE
30 NOV 04
N.W.T.

Scale 1:2500

25 0 25 50 75 100 125 150
metres

ATAC Resources Ltd.

INDUCED POLARIZATION SURVEY

Nicki Grid

Line 400E

Date: 7/10/2004

Interpretation:

Aurora Geosciences Ltd.

YUKON MINERAL RESOURCES
PO BOX 2703
WHITEHORSE, YUKON Y1A 2C6

Pseudo Section Plot
3+00 E

Pole-Dipole Array

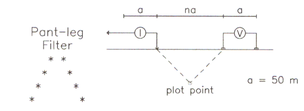

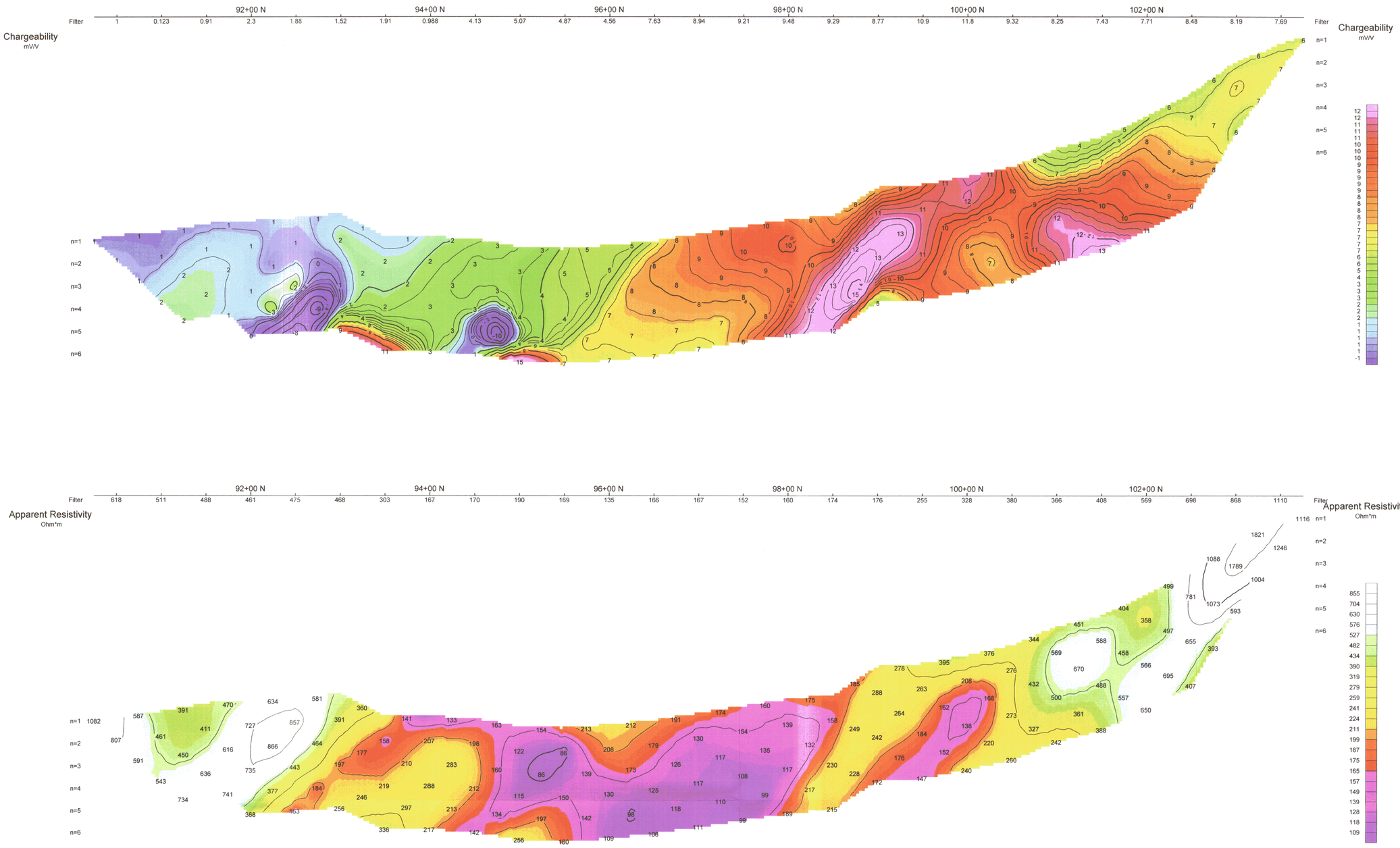

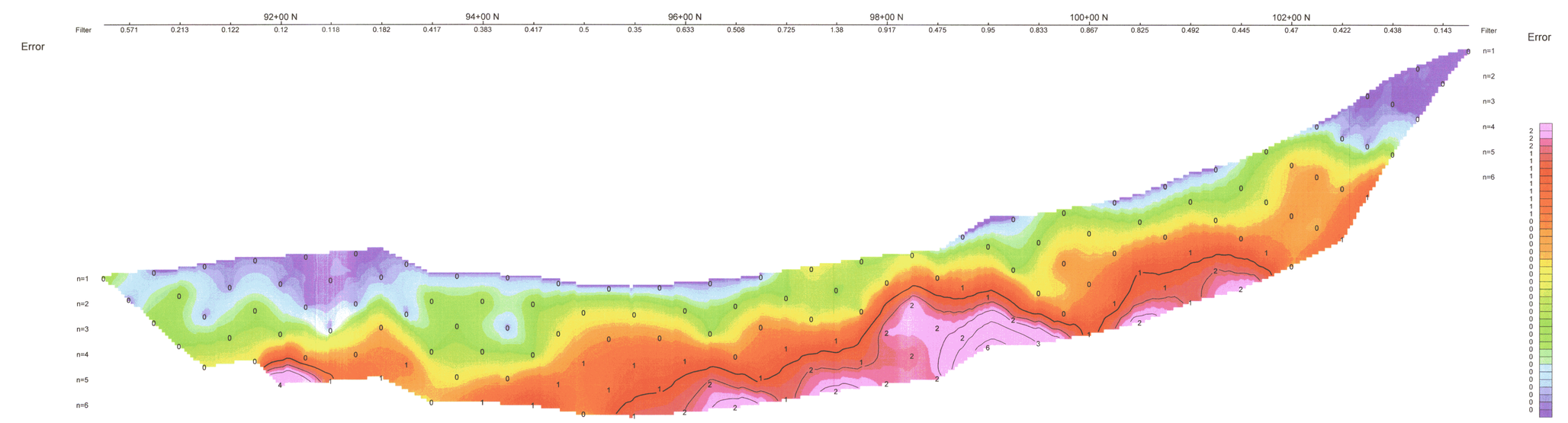

Logarithmic Contours 1, 1.5, 2, 3, 5, 7.5, 10, . . .

INTERPRETATION

- ■ Strong increase in polarization accompanied by marked decrease in resistivity.
- □ Well defined increase in polarization without marked resistivity decrease.
- □ Poorly defined polarization increase with no resistivity signature.
- ▼ Low resistivity feature.

094527

REGISTERED PROFESSIONAL GEOPHYSICIST
M. A. POWER
LICENSEE
30/JUN/04
N.W.T.

Scale 1:2500

25 0 25 50 75 100 125 150
metres

ATAC Resources Ltd.

INDUCED POLARIZATION SURVEY
Nicki Grid
Line 300E

Date: 7/10/2004
Interpretation:

Aurora Geosciences Ltd.

Pseudo Section Plot

2+00 E

Pole-Dipole Array

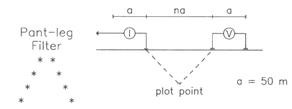

Logarithmic Contours 1, 1.5, 2, 3, 5, 7.5, 10, . . .

INTERPRETATION

- ■ Strong increase in polarization accompanied by marked decrease in resistivity.
- ▣ Well defined increase in polarization without marked resistivity decrease.
- □ Poorly defined polarization increase with no resistivity signature.
- ▼ Low resistivity feature.

REGISTERED PROFESSIONAL GEOPHYSICIST
M.A. POWER
LICENSEE
BONNOVY
N.W.T.

094527

Scale 1:2500

25 0 25 50 75 100 125 150
metres

ATAC Resources Ltd.

INDUCED POLARIZATION SURVEY
Nicki Grid
Line 200E

Date: 7/10/2004
Interpretation:

Aurora Geosciences Ltd.

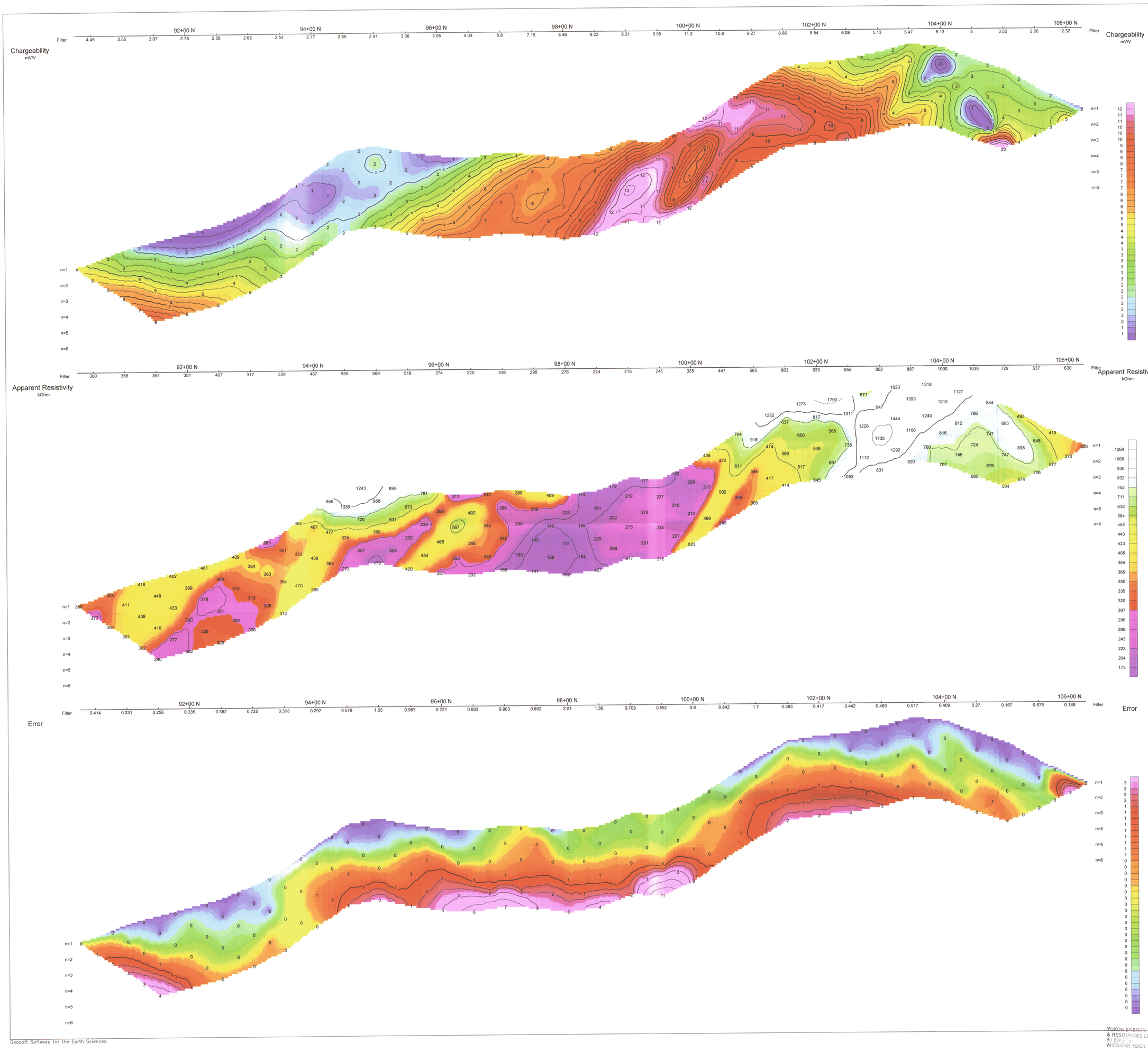

Pseudo Section Plot

1+00 E

Pole-Dipole Array

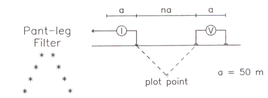

Logarithmic Contours 1, 1.5, 2, 3, 5, 7.5, 10, . . .

INTERPRETATION

- ■ Strong increase in polarization accompanied by marked decrease in resistivity.
- □ Well defined increase in polarization without marked resistivity decrease.
- □ Poorly defined polarization increase with no resistivity signature.
- ▼ Low resistivity feature.

REGISTERED PROFESSIONAL GEOPHYSICIST
M. A. POWER
LICENSEE
BONNYVILLE
N.W.T.

09452

Scale 1:2500

25 0 25 50 75 100 125 150
metres

ATAC Resources Ltd.

INDUCED POLARIZATION SURVEY
Nicki Grid
Line 100E

Date: 7/10/2004
Interpretation:

Aurora Geosciences Ltd.